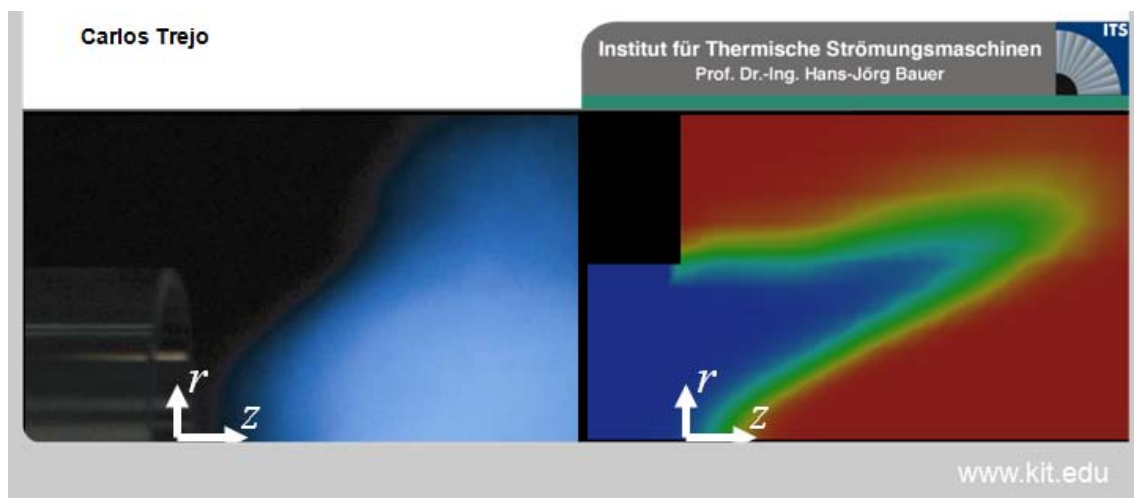


# Numerical Investigation of the Aerodynamic Influence of Combustion on the Vortex Breakdown

With OpenFOAM

Carlos Trejo Velasco

7/5/2010



# Numerical Investigation of the Aerodynamic Influence of Combustion on the Vortex Breakdown

## 1 Introduction

In our global society there is and there will also be in future a strong demand for the service of combustion engines. In the pursuit to improve such engines, making their operation more and more environmentally friendly has become a priority during the recent 20 years. Consequently engineers have improved the design of the complete engine to increase efficiency. But then, at given parameters for the thermodynamic cycle process, the engine emissions solely depend on the quality of the combustion system design and, if existent, the exhaust after treatment. Ideal combustion systems operate at a maximum of stability, a maximum of power density, and a minimum of emissions. Technical systems are never ideal, and the optimization of all three aspects is difficult because usually a measure to improve one deteriorates at least one of the others. Sometimes improvement of the combustion process is not feasible any more by an optimization of the system design but by a change of the system concept. This way scientists, technicians and engineers have come from jet flames to swirl flames and from diffusion flames to partially premixed flames.

The next generation flames, promising reduced emissions, are lean premixed flames. But these flames are prone to instabilities like thermo-acoustic oscillations, blow off and flashback into premixing zones. One type of flashback into premixing zones occurs due to the propagation of the axial recirculation zone in upstream direction into the premixing zone. The relocation of the recirculation zone is caused by the aerodynamic influence of the flame on the swirl flow. The related flashback is known as “flashback caused by combustion induced vortex breakdown” and has yet caused problems in premixing burners for industrial gas turbines. The mechanism of interaction between flame and swirl flow in this type of flashback is still not fully understood. But in order to design combustors for save premixed swirl flames it is necessary to resolve this lack of understanding. Currently this phenomenon is under experimental investigation at the Institute of Thermal Turbomachinery at the KIT in Germany.

This work supports the experimental investigation with insights into the aerodynamic interaction of a flame and a swirl flow obtained through numerical simulation of the reacting swirl flow. The goal is first, to gain a greater understanding of the combustion aerodynamics of swirl stabilized flames in general and second, to investigate the aerodynamic influence of a swirl stabilized flame on the shape and the position of the axial recirculation zone. The principal idea of this work is to build a numerical model that gives the opportunity to study the interaction of flow with a free flame and with a flame fixed in space. The purpose of the fixed flame is to identify the pure influence of the flame on the flow without influence of the flow on the flame. The main findings of this work are: First, at a critical level of swirl one can observe a transition between a flame that is mainly stabilized by the axial recirculation zone and a flame that is mainly stabilized by the vortex in the “back step” corner of the cross section jump at the entry of the combustion chamber. Second, variations of the thickness, the axial position and the angle of the flame front have indeed an effect on the axial position and the shape of the axial recirculation zone of the swirl flow.

## 2 Basics of Reacting Swirl Flows

### 2.1 Swirl Flows

Many natural and technical flows are swirl flows. Swirl flows are characterized by circumferential velocity and the according angular momentum both related to the axis of rotation. The appropriate coordinate system is cylindrical, with the radial coordinate  $r$ , the circumferential coordinate  $\phi$ , and the axial coordinate  $z$ . Accordingly the radial, circumferential and axial velocities are  $u$ ,  $v$  and  $w$  respectively. The type of swirl flow depends solely on the radial profile of the circumferential velocity  $v$ . The two most important types of swirl flows are the potential vortex ( $vr = \text{const}$ ) and the rigid body rotation ( $v = r \cdot \text{const}$ ). The combination of both, rigid body rotation for  $r < r_{\text{core}}$  and potential vortex for  $r > r_{\text{core}}$ , is the so called Rancine vortex. The swirl flows used in this study are also Rancine vortexes.

Understanding the aerodynamics of swirl flows is much harder compared to the understanding of jet flows because in swirl flows, as in all flows where the streamlines follow curvilinear coordinates, the pressure gradient has an additional component perpendicular to the streamlines. We are used to the fact, that the pressure gradient is in line with the acceleration vector. But usually it is assumed, that this acceleration leads to a change in the magnitude of the velocity vector. It usually does. But in curvilinear coordinates, acceleration can be related also to a change in the direction of the velocity vector. In a steady swirl flow without radial fluid motion the radial component of the pressure gradient is:

$$\frac{dp}{dr} = \rho \frac{v^2}{r}$$

This pressure gradient becomes most obvious, when rotating a pot with water around its center axis, which is aligned with the gravitational acceleration. The water level rises with radius, according to the rise in static pressure. Similarly this radial pressure gradient occurs also in swirl flows where gravity can be neglected. Due to this pressure gradient swirl flows can undergo severe transitions, in which velocity profiles change drastically. One transition which commonly occurs if a flow with sufficient swirl is exposed to a smooth or sudden increase in cross section area is the “vortex breakdown”. In this transition the swirl flow expands in radial direction and stagnates on its axis. A recirculation zone establishes downstream the axial stagnation point. This recirculation zone can then be used as a flame holder to stabilize a flame inside a high speed swirl flow. This is the basic concept of swirl stabilization as it is applied in technical combustion systems found e.g. in gas turbines.

### 2.2 Aerodynamic Influence of Combustion

A flame is the zone, in which the heat releasing oxidation reaction between the fuel and the oxygen (usually available as a dilution of oxygen and air) takes place. As the fluid crosses the flame front, the heat release causes a rise of the fluid temperature and a drop of the fluid density. Due to the conservation of mass, the fluid accelerates when crossing the flame front. Taking into account the conservation of momentum, the static pressure drops across the flame front according to the following relation:

$$\Delta p = \rho_u S_t^2 \left( \frac{T_b}{T_u} - 1 \right)$$

Due to this pressure drop across the flame front, a flame does not only change the flow field downstream the flame front, but can also influence the flow field upstream the flame front. This upstream influence of the flame is suspected to cause the propagation of the vortex breakdown transition in upstream direction.

### 3 Characterization of this work

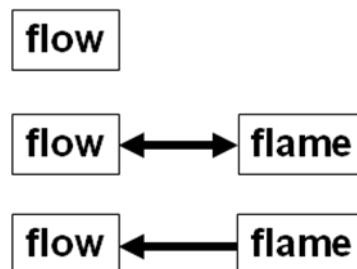
One of the purposes this project serves is the supporting and backing up of certain theories and assumptions drawn from an experiment on the aerodynamic interaction of swirl flames with swirl flows carried out at the “Institut für Thermische Strömungsmaschinen” in the “Karlsruhe institute of technology”.

The goal was to obtain qualitatively correct predictions of the interaction between the flow and the flame for different situations. We were walking on unknown territory, which is why our learning mechanism was “trial and error”. This demands for a great number of simulations, which can only be achieved if the turnover time is low. We were not looking for a very accurate tool, but rather, for a very fast one.

This is what led us to choose a two dimensional RANS (Reynolds Averaged Navier Stokes) model, with a relatively coarse mesh.

#### Procedure:

1. Model of the non-reacting flow
2. Model of the reacting flow with a free flame
3. Model of the reacting flow with a fixed flame  
(no influence of the flow on the flame)



The first step was to model the cold flow. Then, this model was extended, and combustion was implemented into it. We were now in a position to study the interaction between the flame and the flow. The problem with this is that it was impossible to isolate the influence of the flame on the flow, for there is always a feedback influence of the flow on the flame. We decided to break this feedback loop. This was achieved by modifying the solver, so that the flame would be fixed in space. After being initialized according to our needs, this flames remained unchanged throughout the simulation, which eliminates the influence of the flow on the flame.

### 3.1 The flow and the flame

#### 3.1.1 The Flow Field

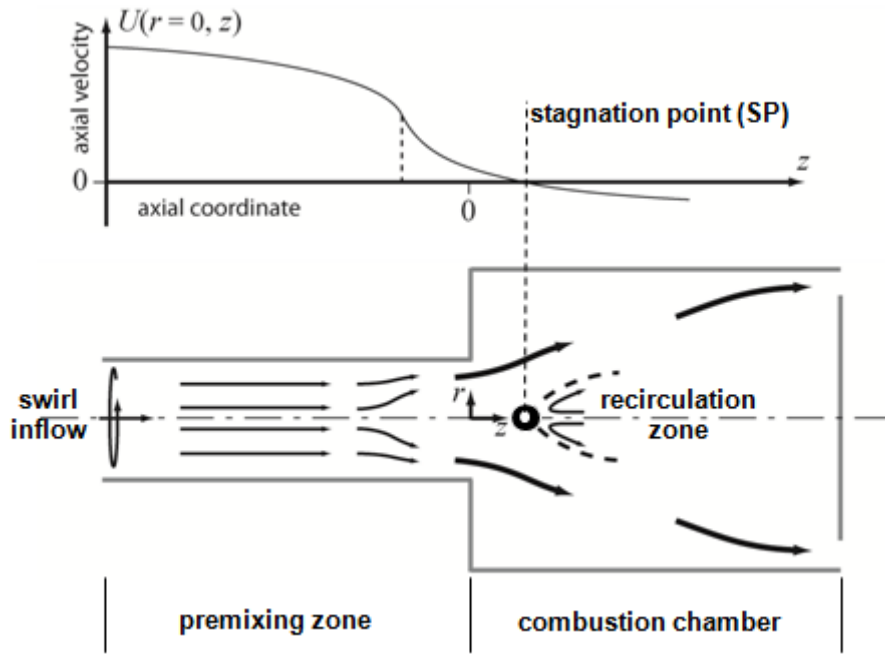


Figure 1

The geometry of the problem, as can be seen, is quite simple. It is made up of two cylinders: the premixing zone, and the combustion chamber. The flow enters the premixing zone with swirl, which causes it to expand radially when it reaches the combustion chamber. This creates a recirculation zone at the axis.

In the axial velocity distribution along the axis, the stagnation point can be appreciated, which is the point along the axis for which the axial velocity is zero. This point marks the beginning of the recirculation zone, and is the parameter we will be referring to from now on to characterize the flow field.

#### 3.1.2 The Flame

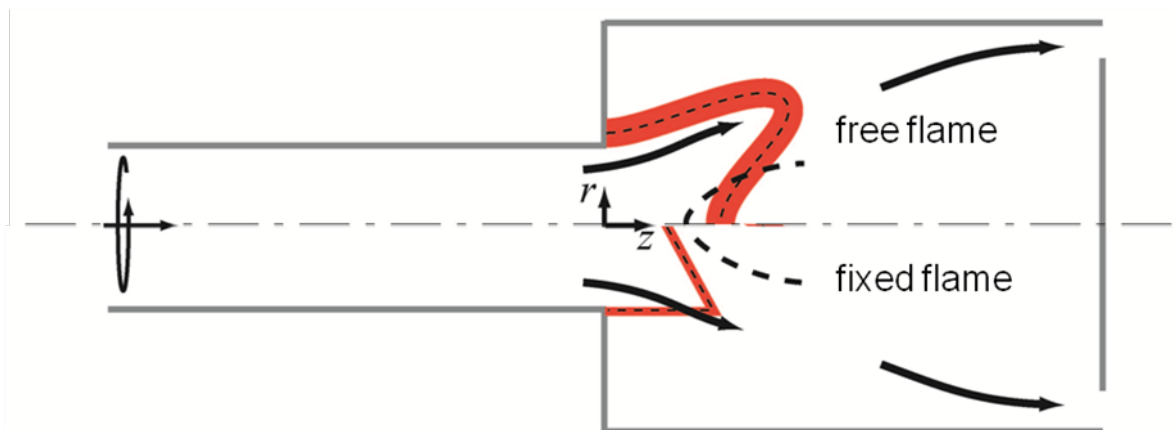


Figure 2

As mentioned earlier on, throughout this study we have been working with two types of flames: the free flame, which adapts to the flow, and the fixed flame, over which we have total control. In this flame we can tweak certain parameters to study their influence on the

flow field, such as the axial position of the flame front, its thickness, or the angle between it and the axis.

### 3.2 The numerical setup

#### 3.2.1 The 2d simplification

From the beginning, we chose a 2D axisymmetric simplification of the geometry, which is shown in Figure 2

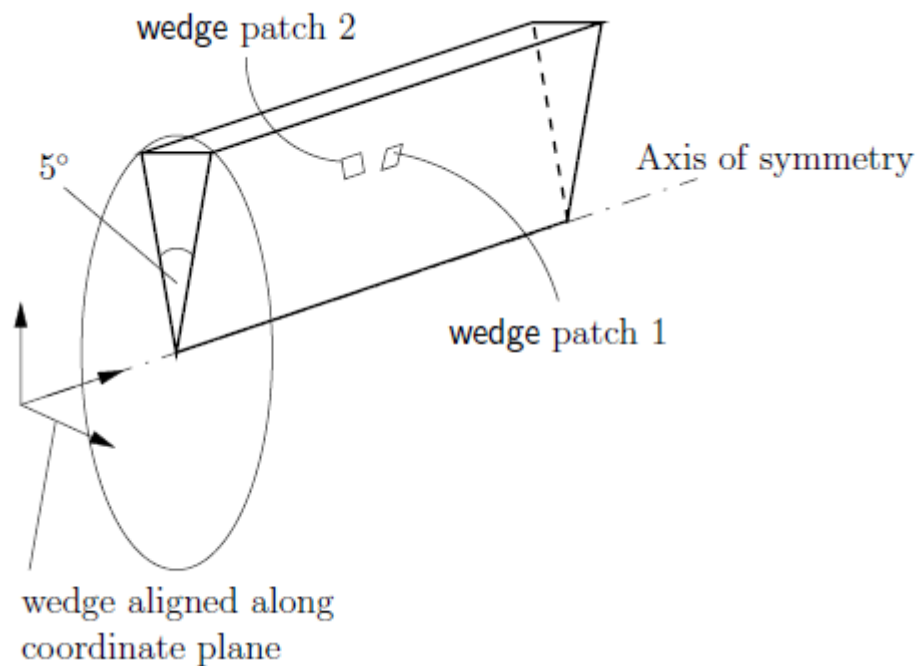


Figure 3

#### 3.2.2 The mesh

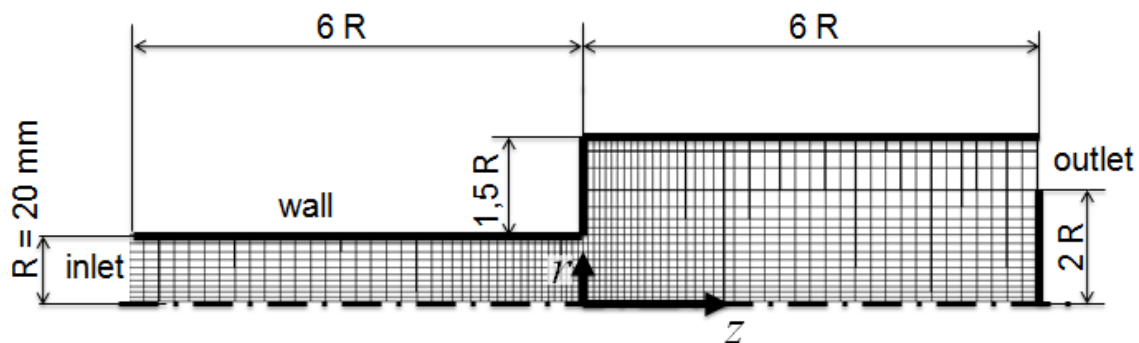


Figure 4

There are certain zones with a greater demand for accuracy, such as the elbow or the axis. At these points, the mesh has consequently been refined. To increase the stability of the simulation, a wall was added at the outlet as can be seen in the Figure 4. This is usual in this type of simulation, since the reverse flow that can take place at these points deteriorates the stability of the simulation.

### 3.2.3 The solver- XiFoam from OpenFOAM

The CFD (computational fluid dynamics) code chosen has been OpenFOAM all along, an open source program, whose solvers can be modified. This was of crucial importance for the study.

The solver is “XiFoam”, a compressible solver that simulates combustion through a progress value

### 3.2.4 The turbulent model- RAS

Reynolds-averaged stress (RAS) turbulence models are used to solve for the mean flow behaviour and calculate the statistics of the fluctuations.

The model used in this case was the standard  $k$ - $\epsilon$ , which initial values had to be estimated by hand (to initialize the calculations, some such as epsilon or  $k$  change in time), using the following expressions:

$$k = \frac{3}{2}(UI)^2,$$

where  $I$  is the initial turbulence intensity [%] given below, and

$U$  is the initial velocity magnitude;

$$\epsilon = c_{\mu}^{3/4} k^{3/2} l^{-1}.$$

Here  $l$  is the turbulence or eddy length scale, give below, and

$c_{\mu}$  is a  $k$ - $\epsilon$  model parameter whose value is typically given as 0.09;

$$I = 0.16Re^{-1/8}.$$

Further  $Re$  is the Reynolds number

$$l = 0.07L,$$

with  $L$  the characteristic length, the radius in this case.

### 3.2.5 The combustion model

The combustion model we chose was the “Flame Surface Density model” developed by Weller, which takes into account the greater surface of the “instantaneous” flame due to its fluctuating wrinkling. The heat release is modeled following a simplistic approach: the temperature distribution follows the burned/unburned (progress variable) distribution.

### 3.2.6 The boundary conditions

The boundary conditions were chosen as follows:

	Inlet	Walls	Outlet
Velocity	Rankine vortex	Slip	zeroGradient
Pressure	zeroGradient	zeroGradient	102000 Pa
Temperature	300K	zeroGradient	zeroGradient

The velocity at the inlet is made up of two components, the axial component, which is constant throughout the inlet, and the circumferential component, which has the shape of a Rankine vortex along the radius.

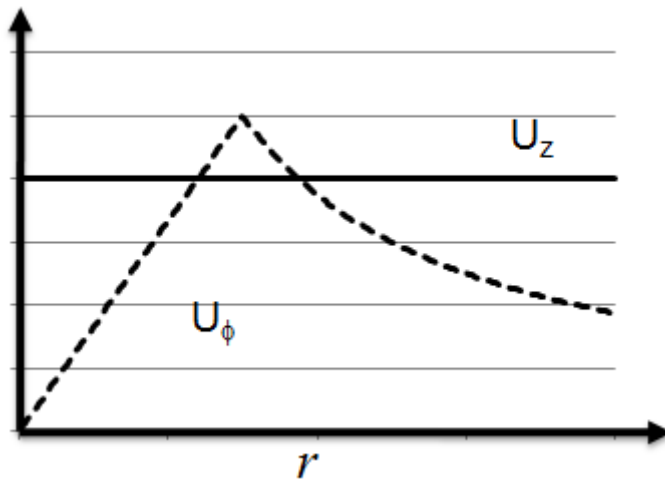


Figure 5

The temperature was fixed at the inlet, the pressure at the outlet.

### 3.3 The strategy developed- the cases run

The solvers used in this study are the following:

- *icoFoam*: unsteady-state, incompressible solver
- *simpleFoam*: steady-state, incompressible solver
- *XiFoam*: unsteady-state compressible solver which allows for combustion
- *yourXiFoam*: unsteady-state modified version of XiFoam in which the flame stays at its initial position.

The following diagram shows the the structure that was followed from the very beginning, with the incompressible solver *icoFoam*, until the very last one with the fixed flame and *yourXiFoam*.

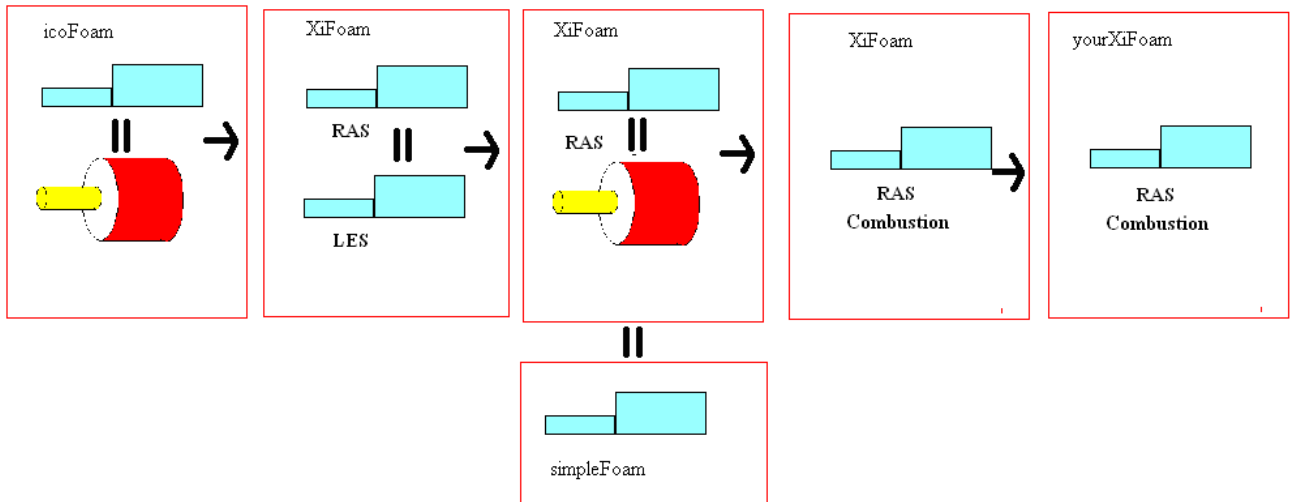


Figure 6

The whole process is presented in the following pages. Since it is so long, a summary is included so as not to lose overview over the whole process.

1. The incompressible flow field (without turbulence)
2. The compressible flow field
  - 2.1. LES
  - 2.2. RAS
3. Comparing to an incompressible, turbulent flow
4. Introducing combustion-the fixed flame
  - 4.1. The combustionProperties dictionary
  - 4.2. Lighting up the flame
    - 4.2.1. The spark
    - 4.2.2. The initial flame front
5. The fixed flame

### 3.3.1 The incompressible flow field (without turbulence)

The first step was to set up an initial case. For this purpose, we set up a 3D model as well as a 2D one. *icoFoam* solves two variables, pressure and velocity.

The pressure has to be set at one point. Fixing it to a certain value at the inlet and outlet led to instabilities. It was also noticed that fixing it at the outlet was a much more stable (and realistic) approach. The outlet pressure was fixed to 100000Pa, this value is not of great importance in *icoFoam*. The rest of the boundary conditions were set to *zeroGradient*.

The velocity field was set using the *funkySetFields* utility. This very practical utility sets fields for any of the variables of the program in space, namely boundary and initial conditions. Although in 2D it was not absolutely essential, later on it turned out we could not have lived without it. Here is a small script showing its use:

```

FoamFile
{
  version      2.0;
  format       ascii;

  root         "/.automount/werner/Werner/bgschaid/bgschaid-foamStuff/DepositionTests";
  case         "neutralTest";
  instance     "system";
  local        "";

  class        dictionary;
  object       funkySetFieldsDict;
}

expressions
(
  .   U_in
  .   {
  .   .   keep Patches;
  .   .   field U;
  .   .   valuePatches (inlet);
  .   // this fixes the boundary condition in the inlet
  .   .   expression "vector(0,0,0)";
  .   .   expression "vector(10,0,pos().y*2666.666667/2)";
  .   .   condition "(pos().y<0.0075) && (pos().y>=0)";
  .   .   //expression "vector(10,0,(2666.666667*0.0075*0.0075/2)/(pos().y))";
  .   .   //condition "(pos().y<0.020) && (pos().y>=0.0075)";
  .   //only one expression can be executed at a time, that's the reason why the other one is behind comments
  .   }
);

```

Figure 7

The velocity field chosen for the circumferential speed follows a Rankine profile, whereas the axial component is constant and equal ten throughout the tube, and the axial one equals zero.

In the walls, various options were tried out. The possibilities range from *slip*, where the tangential component of the speed remains unaffected by the presence of the latter, to *fixedValue (0 0 0)*. In between, there is all the range of options to be set with the command *wallFunction*, between zero and one.

In the end, it was decided the influence of the boundary layer could be neglected, and since there was computational time to be saved by choosing *slip*, this option prevailed.

The purpose of this first very basic simulation was not to be exact, but to see if the Combustion Induced Vortex Breakdown phenomenon actually happened in the 2D simulation.

The velocity profile of a 2 and 3D simulations after reaching a stable value is shown in Figure 8

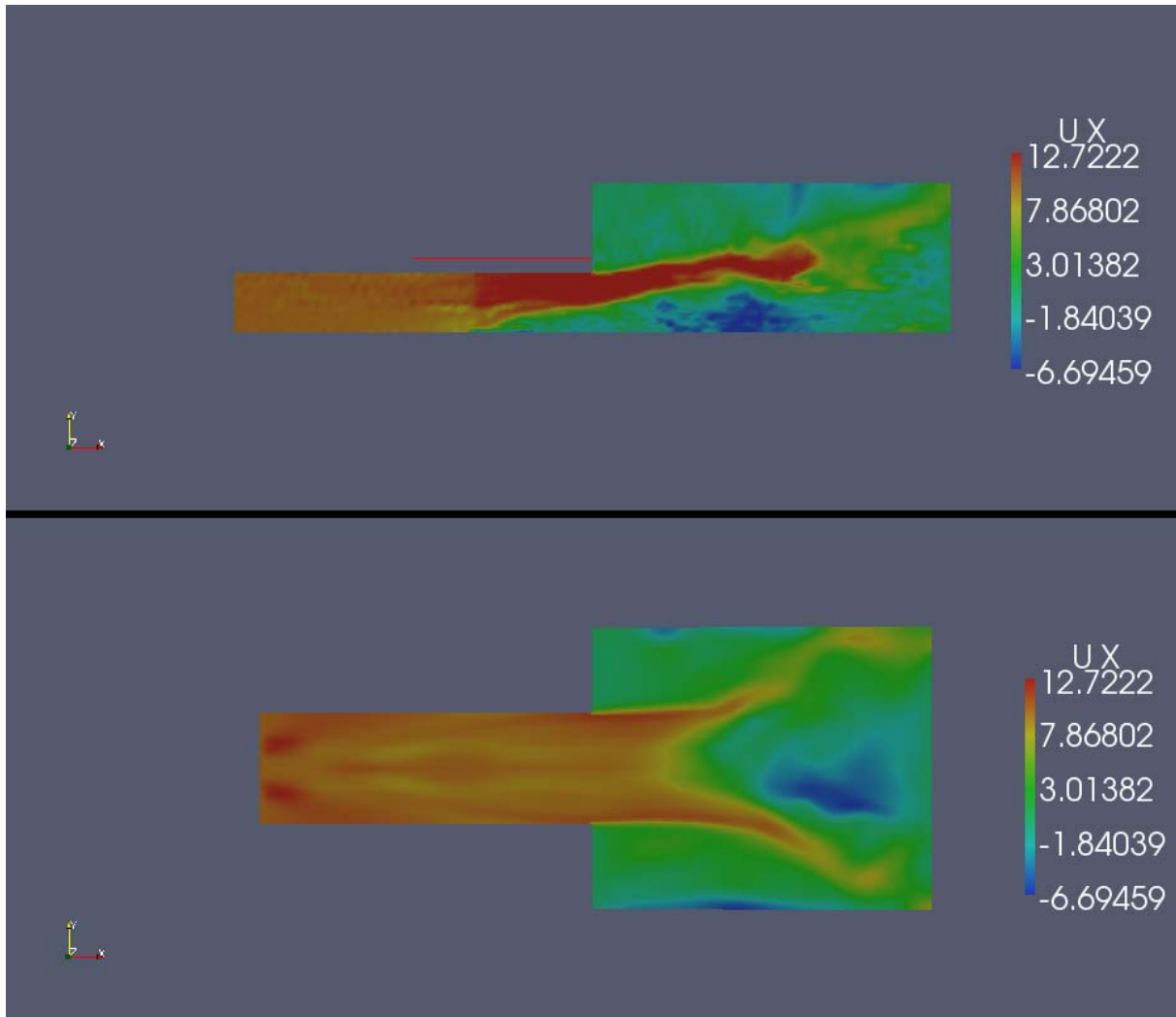


Figure 8.

The field below belongs to a slice of the 3D body taken right through the middle. It can be appreciated that there are differences in the velocity fields, however, our goal here was not precision, but verifying that it would be possible to simulate in 2D as well. This lack of exact of accuracy may respond to the lack of turbulent simulation: in this case, the Reynolds number was far too high to accept laminar modelling.

Afterwards, we moved onto the next step, which is working with a compressible solver: XiFoam

### 3.3.2 The compressible, turbulent flow

As mentioned before, XiFoam is a compressible solver which allows for premixed/partially premixed combustion with turbulence modelling.

Our problem having a very high Reynolds number, it is infeasible to bear the huge cost of solving the turbulent behaviour directly. Turbulence has to be statistically modelled, this can be done at two levels: RAS and LES

## LES- Large eddy Simulation

A common deduction of Kolmogorov's (1941) famous theory of self similarity is that large eddies of the flow are dependent on the flow geometry, while smaller eddies are self similar and have a universal character. For this reason, it became a practice to solve only for the large eddies explicitly, and model the effect of the smaller and more universal eddies on the larger ones. Thus, in LES the large scale motions of the flow are calculated, while the effect of the smaller universal scales (the so called sub-grid scales) are modeled using a sub-grid scale (SGS) model. In practical implementations, one is required to solve the filtered Navier-Stokes equations with an additional sub-grid scale stress term. The most commonly used SGS models are the Smagorinsky model and its dynamic variants. They compensate for the unresolved turbulent scales through the addition of an "eddy viscosity" into the governing equations. This approach delivers more detail than RAS modelling at a higher computational cost, thus standing between direct numerical simulation and the latter.

LES simulation, however, works only to a certain extent in our wedge-2D approach, since the whirls need a 3D geometry to develop.

In order for this simulation type to work, there needs to be initial turbulence at the inlet, which can be taken care of through the *turbulentInlet* option:

```
inlet
{
    type          turbulentInlet;
    referenceField nonuniform List<vector>
10
(
(10 0 4.02061),
(10 0 4.68873),
(10 0 5.5411),
(10 0 6.66212),
(10 0 8.19678),
(10 0 9.60002),
(10 0 7.19667),
(10 0 4.97958),
(10 0 2.95022),
(10 0 1.22684)
);
    fluctuationScale (0.037 0 0.037);
}
```

The turbulent intensity, which is the input for *fluctuationScale*, was calculated following the expression :

$$I = 0.16Re^{-1/8}.$$

The whirls that should appear in a URANS (non-stationary Reynolds-averaged Navier-Stokes) are nowhere to be seen, as shown in Figure 9

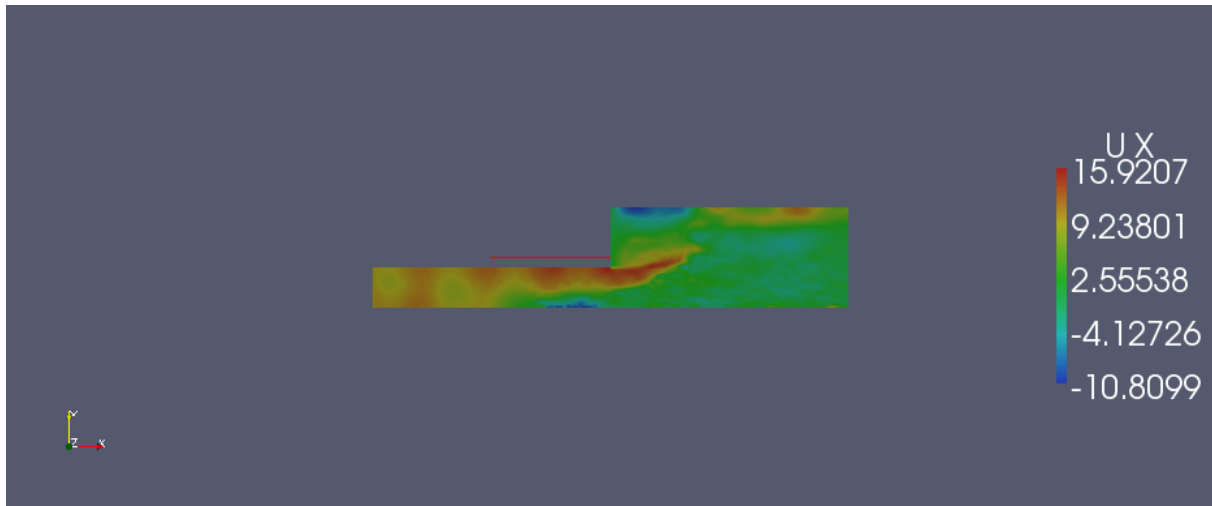


Figure 9

A 3D simulation would be needed, and although feasible, this would drastically raise the turnover time (two orders of magnitude because of the 3D geometry, almost one order of magnitude because of the more time-consuming character of LES). Since the purpose of this study is not precision, but studying particularities of the CIVB phenomenon, this option was ruled out

### **RAS – Reynolds-averaged Stress**

This model, which has already been explained before, for it is a setting that was used all along most of the simulations, prevailed for its lower turnover time, and because it was easier to understand.

The results of 2D and 3D simulations with this turbulence modelling are shown in Figure 10

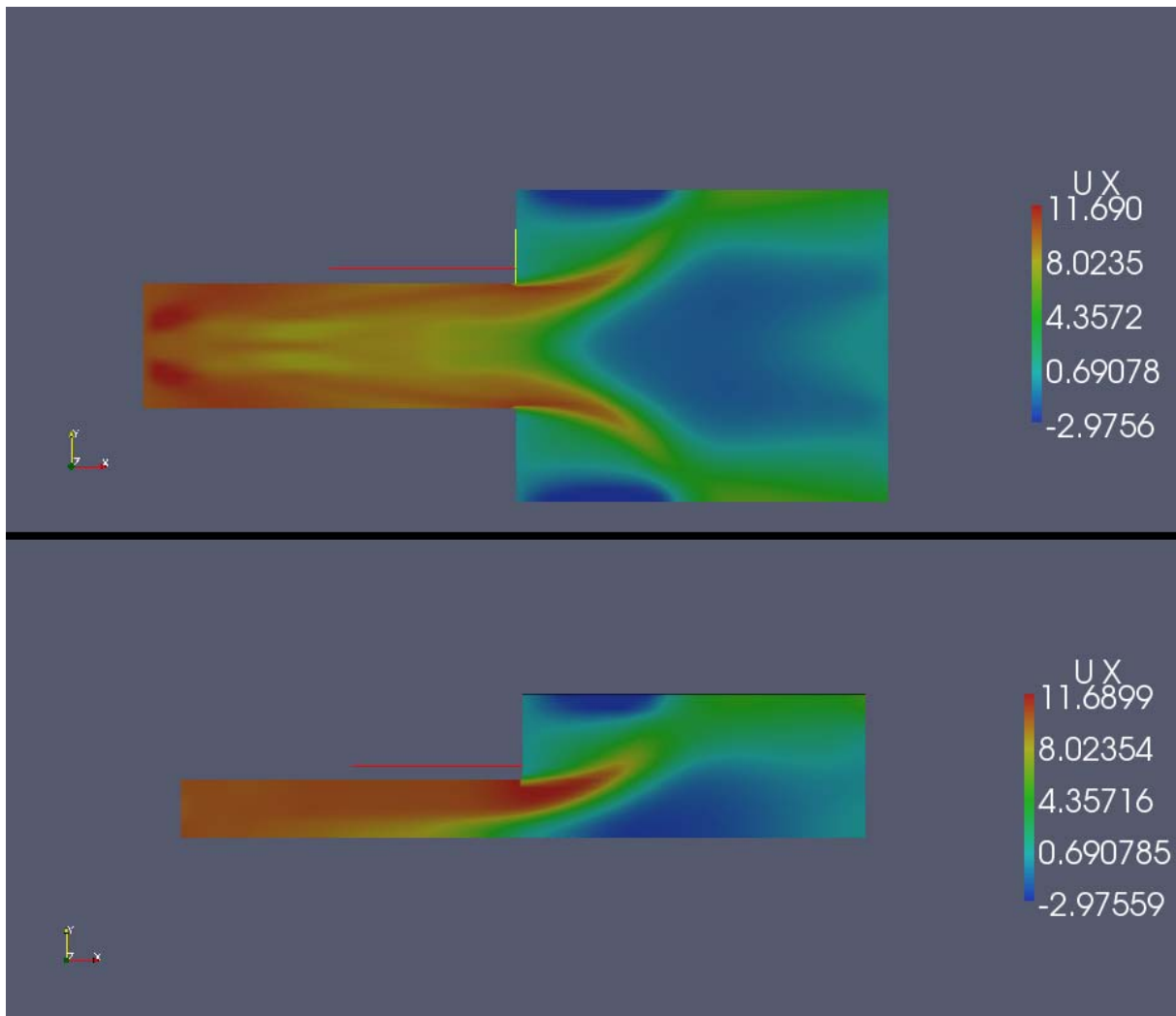


Figure 10

The curious axial velocity at the inlet of the 3D model may be a hint on the velocity at the inlet, which could possibly have been set in an incorrect way

### 3.3.3 comparison to an incompressible, turbulent flow.

Since one solver alone can not be completely trusted, we thought it convenient to compare results with those of simulations using other solvers. Fortunately, the “Institut für thermische Strömungsmaschinen” is quite big, so that there happened to be another researcher working on the same phenomenon, using a different solver, *simpleFoam*, a steady-state solver for incompressible, turbulent flow. The results are shown in Figure 11

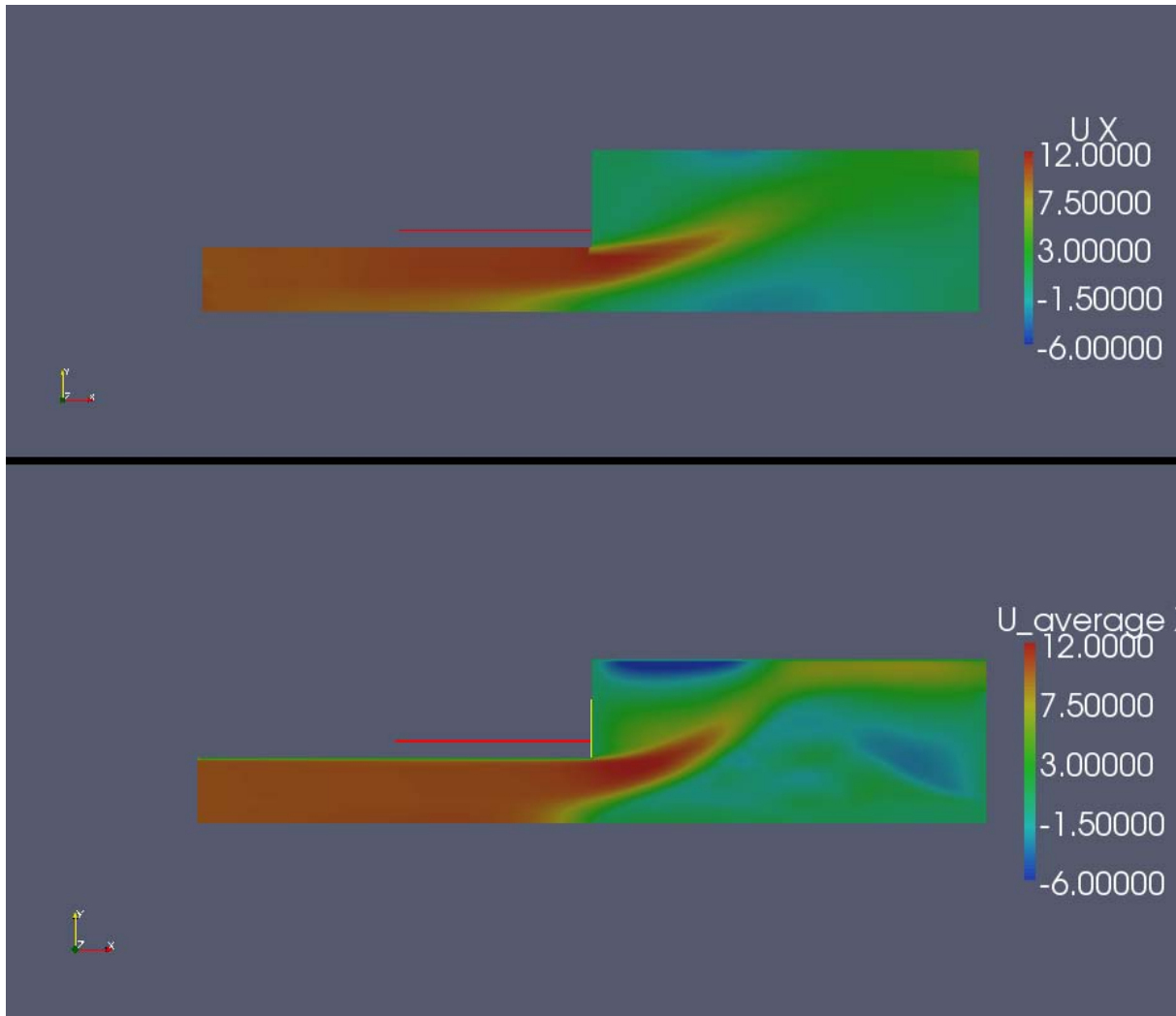


Figure 11

The upper simulation was carried out with XiFoam, the lower with simpleFoam. There is a certain accordance, although some differences as well. The vortex breakdown takes up more space in simpleFoam, and the recirculation at the walls is more pronounced. However, the stagnation point is in the same place for both models

### 3.4 Introducing combustion-the free flame

#### 3.4.1 The combustionProperties dictionary

Plenty of options related to combustion can be set in this dictionary. The parameters we set are the following:

- Fuel: Methane. This sets the initial Gulderson coefficients
- Flame speed: It is important to realise that the flame speed for most hydrocarbon fuels is very similar (around 0.4m/s). This is because all hydrocarbons are quickly pyrolysed to smaller sized molecules before combustion and hence behave in a similar manner.

- Equivalence Ratio: 0.6

```

FoamFile
{
  version      2.0;
  format       ascii;
  class        dictionary;
  location     "constant";
  object       combustionProperties;
}
// *****

laminarFlameSpeedCorrelation constant;

fuel          Methane;

Su            Su [0 1 -1 0 0 0 0] 0.4;

SuModel       transport;

equivalenceRatio equivalenceRatio [0 0 0 0 0 0 0] 0.6;

sigmaExt      sigmaExt [0 0 -1 0 0 0 0] 338;

XiModel       transport;

XiCoef        XiCoef [0 0 0 0 0 0 0] 0.62;

XiShapeCoef   XiShapeCoef [0 0 0 0 0 0 0] 1;

uPrimeCoef    uPrimeCoef [0 0 0 0 0 0 0] 1;

GuldersCoeffs
{
  Methane
  {
    W          0.422;
    eta        0.15;
    xi         5.18;
    alpha      2;
    beta       -0.5;
    f          2.3;
  }
}

```

Figure 12

### 3.4.2 Lighting up the flame

There were two available ways to do this: either through lighting up a spark, or through a gradient in the progress variable  $b$  which would simulate an artificial flame.

#### The spark

This was the first option that was tried.

In the *combustionProperties* dictionary, the spark was defined as can be seen in Figure 13:

```

ignite    yes;

ignitionSites
(
  {
    location (0.15 0.002 0);
    diameter 0.03;
    start 0;
    duration 0.1;
    strength 50;
  }
);

ignitionSphereFraction 0;

ignitionThickness ignitionThickness [0 1 0 0 0 0] 0.001;

```

Figure 13

Although variations in these parameters were tried over and over, no satisfactory results could be pulled out of this procedure. The flame either burned too violently, leading to instant flashback at its best and calculations breaking off at its worst, or did not light up at all. This rather “uncontrollable” procedure had to be turned down.

### The initial flame front

There was no big need for precision as this is only the initial solution for the flame to develop itself. Setting a sudden transition from unburned to burned led to instabilities, so the thickness was increased to lower the gradient.

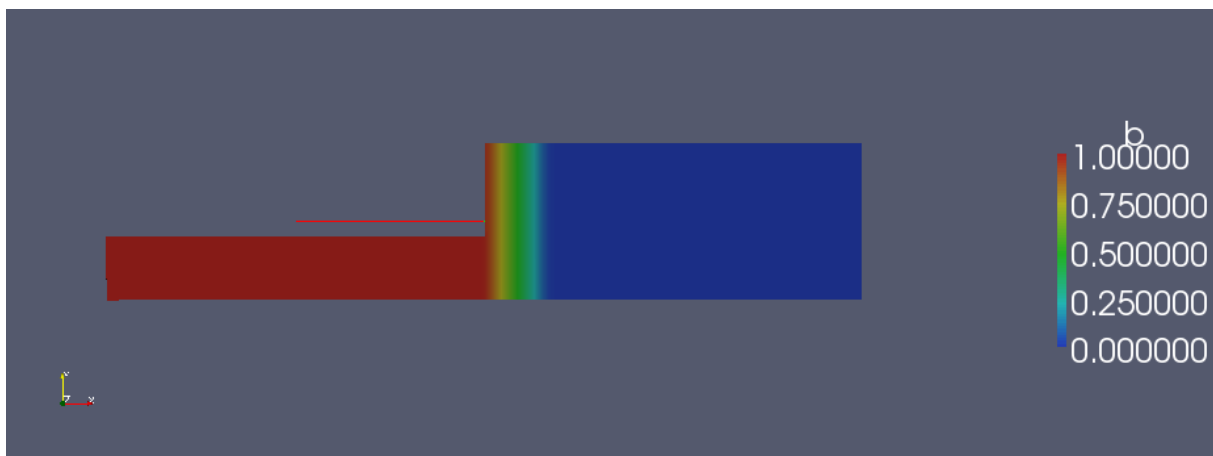


Figure 14

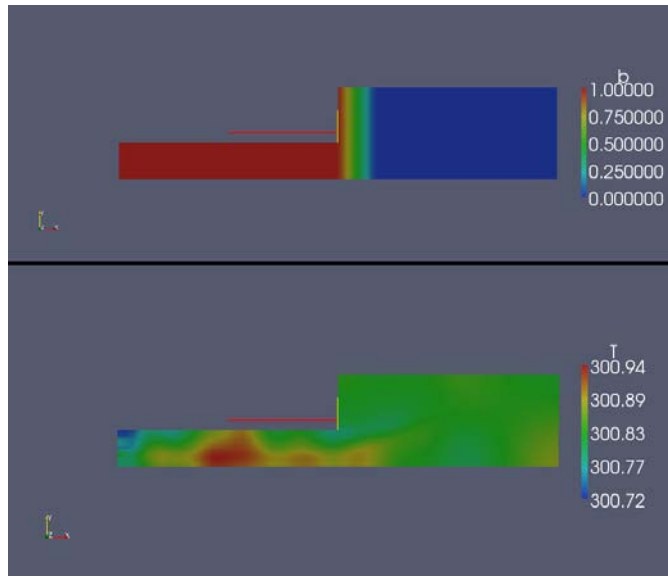


Figure15  $t=0$

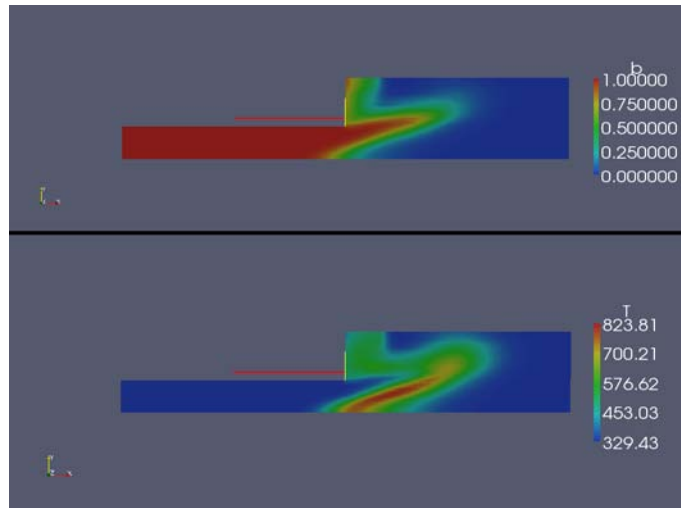


Figure 16  $t=0.02s$

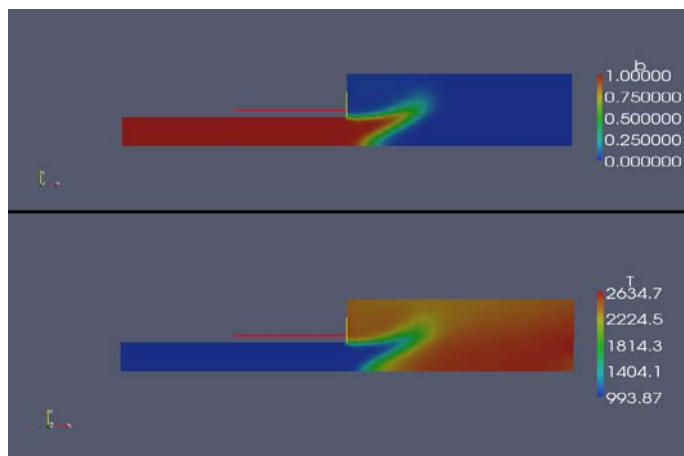


Figure 17  $t=0.15s$

It can be seen in Figure 17 , that the temperatures are higher than they should. This is because of the before mentioned problem of setting the temperature boundary condition at the inlet as *zeroGradient*.

### 3.5 The fixed flame

This was achieved by modifying the solver *XiFoam*. A new solver called *yourXiFoam* was created, to which a small but crucial modification was done in the *bEqn* file.

```
// Create b equation
// ~~~~~
fvScalarMatrix bEqn
(
    fvm::ddt(rho, b)
  + mvConvection->fvmDiv(phi, b)
  + fvm::div(phiSt, b, "div(phiSt,b)")
  - fvm::Sp(fvc::div(phiSt), b)
  - fvm::laplacian(turbulence->alphaEff(), b)
);
```

Figure 18

```
// Create b equation. ddt(b)=0 causes the b field to be stationary and thereby fixes the flame position
// ~~~~~
fvScalarMatrix bEqn
(
    fvm::ddt(b)
.....
);
```

Figure 19

The old equation was replaced by a new one fixing *b* in time. This means, the shape of the flame could be set at wish, with an initial solution using for instance the *funkySetFields* dictionary.

The flame geometry shown in Figure 20 was used in our first tests.

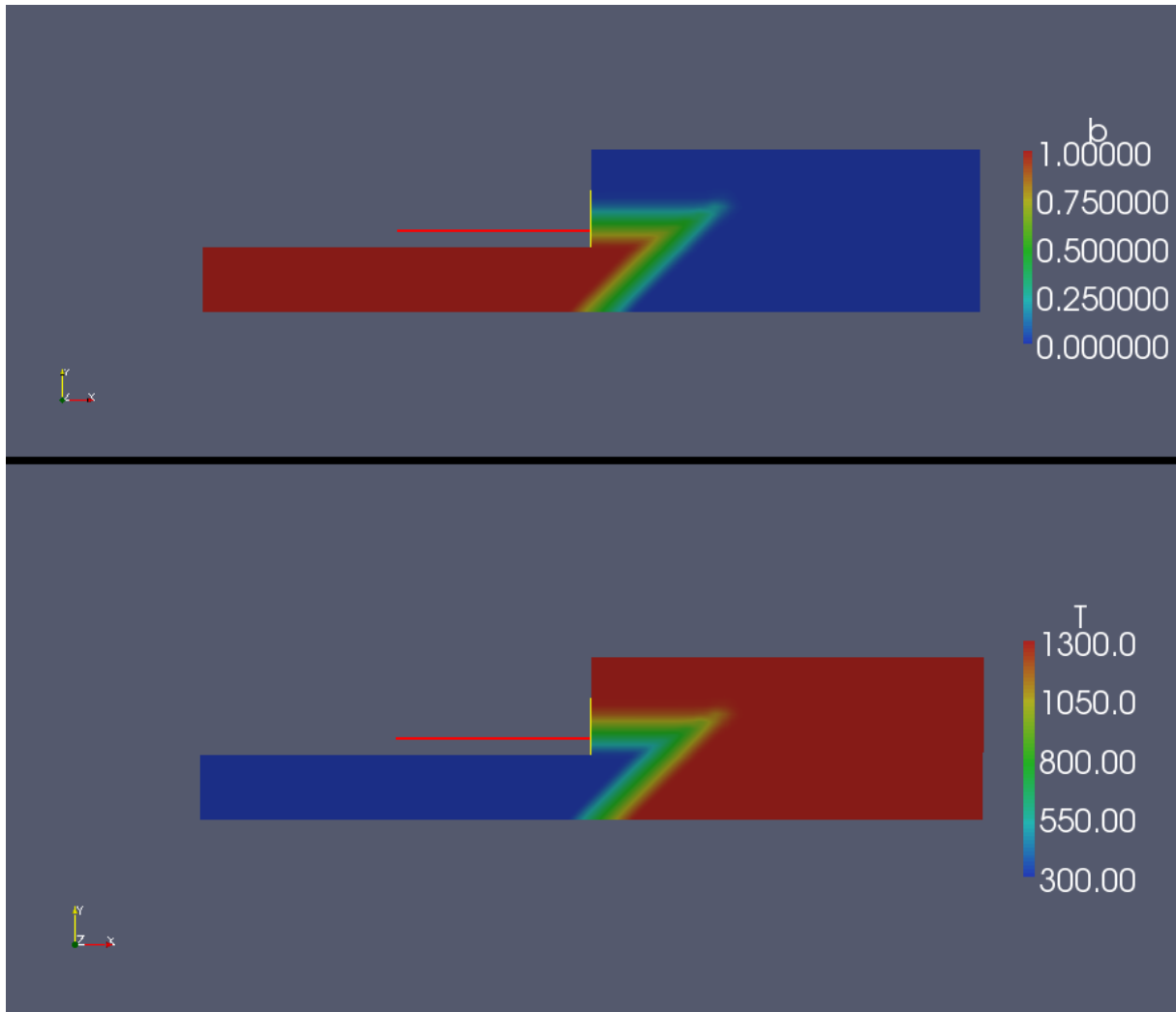


Figure 20

The simulations have been classed here in chronological order with their most relevant parameters (besides the ones which remained constant throughout the study), in the following list, which includes not all simulations, but the most relevant ones:

sim	solver	turb. model	Mesh	init. sol.	flame	pos.	thick-ness	Angle	Max. Circumf. Vel (m/s)	type of sol.
1	icoFoam	-	2D no grading	-	-	-	-	-	10	Start solution
2	icoFoam	-	3D	-	-	-	-	-	10	Start solution
3	icoFoam	-	3D O-grid	-	-	-	-	-	10	comparison
4	icoFoam	-	3D unstruc.	-	-	-	-	-	10	comparison
5	XiFoam	RAS	2D no grading	-	-	-	-	-	10	Start solution
6	XiFoam	LES	2D no grading	-	-	-	-	-	10	comparison
7	XiFoam	RAS	2D grading	-	-	-	-	-	10	Start solution
8	XiFoam	RAS	2D grading	7	-	-	-	-	8	Swirl factor
9	XiFoam	RAS	2D grading	7	-	-	-	-	9	
10	XiFoam	RAS	2D grading	7	-	-	-	-	11	
11	XiFoam	RAS	2D grading	7	-	-	-	-	12	
12	XiFoam	RAS	2D grading	7	-	-	-	-	13	

13	XiFoam	RAS	2D grading	7	-	-	-	-	14	
14	XiFoam	RAS	2D grading	7	-	-	-	-	15	
15	XiFoam	RAS	3D O-grid	-	-	-	-	-	10	
16	simpleFoam	k-Epsilon	2D grading	-	-	-	-	-	10	comparison
17	XiFoam	RAS	2D grading	7	Free	-	-	-	10	Start solution
18	XiFoam	RAS	2D grading	17	Free	-	-	-	8	Swirl factor
19	XiFoam	RAS	2D grading	17	Free	-	-	-	9	
20	XiFoam	RAS	2D grading	17	Free	-	-	-	11	
21	XiFoam	RAS	2D grading	17	Free	-	-	-	12	
22	XiFoam	RAS	2D grading	17	Free	-	-	-	13	
23	XiFoam	RAS	2D grading	17	Free	-	-	-	14	
24	XiFoam	RAS	2D grading	17	Free	-	-	-	15	
25	XiFoam	LES	2D grading	17	Free	-	-	-	10	comparison
26	yourXiFoam	RAS	2D grading *4	17	Fixed	-7	30	33,7°	10	Start solution
27	yourXiFoam	RAS	2D grading *4	26	Fixed	-17	30	33,7°	10	Position
28	yourXiFoam	RAS	2D grading *4	26	Fixed	-27	30	33,7°	10	
29	yourXiFoam	RAS	2D grading *16	26	Fixed	-7	15	33,7°	10	Thickness
30	yourXiFoam	RAS	2D grading *36	26	Fixed	-7	10	33,7°	10	
31	yourXiFoam	RAS	2D grading *4	26	Fixed	-7	30	18,4°	10	Angle
32	yourXiFoam	RAS	2D grading *4	26	Fixed	-7	30	26,6°	10	
33	yourXiFoam	RAS	2D grading *4	26	Fixed	-7	30	45°	10	
34	yourXiFoam	RAS	2D grading *4	26	Fixed	-17	30	26,6°	10	Angle/pos
35	yourXiFoam	RAS	2D grading *4	26	Fixed	-27	30	18,4°	11	

- 2D grading \*4 stands for a 2D mesh with grading with twice as many cells in each direction, so 4 times as many cells in total.
- In the simulations where the flame front thickness was reduced, the cell size was reduced in the same proportion, so as not to become inaccuracies due to a too coarse mesh.

## 5 . The observed aerodynamic influence

The cases from which results were drawn were simulated using a non stationary solver, XiFoam. However, due to the 2D simplification, the whirls which left the the wedge did not re-enter, turning the simulation into a RANS (Reynolds Averaged Navier Stokes). A phenomenom with is present in the real experiment and was missed because of the stationary character of this simulation was the recirculation zone rotating around the axis. Before starting with the results, it should first be cleared that their accuracy is not guaranteed. It is possible, and probable, that the recirculation zone is “underestimated” because of the stationary character of the simulation. The real position of the stagnation point is probably upstream to what has been observed in these simulations.

## 5.1 Model of the non-reacting flow field

The first step was modelling the cold flow field. In Figure 21, the axial velocity can be seen. The scale is adapted to better visualization of the recirculation zones, blue meaning axial velocities of 0m/s or below.

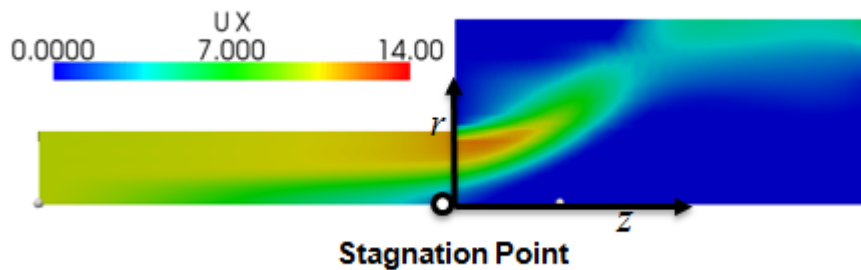


Figure 21

There are two recirculation zones, one in the corner and the other one at the axis, which is the one we are interested in. The stagnation point precedes this recirculation zone upstream.

The swirl factor is a very frequent parameter in this kind of experiment. It is defined as the ratio of swirl momentum flux to axial momentum flux.

$$S = \frac{\dot{D}}{\dot{I}}$$

In our case, the axial momentum flux was left unchanged throughout the study, so variation on the swirl factor corresponds exclusively to variation on the circumferential velocity of the flow at the inlet.

This experiment has been carried out for different swirl factors, which results, characterized by the stagnation point, can be seen in the following graph:

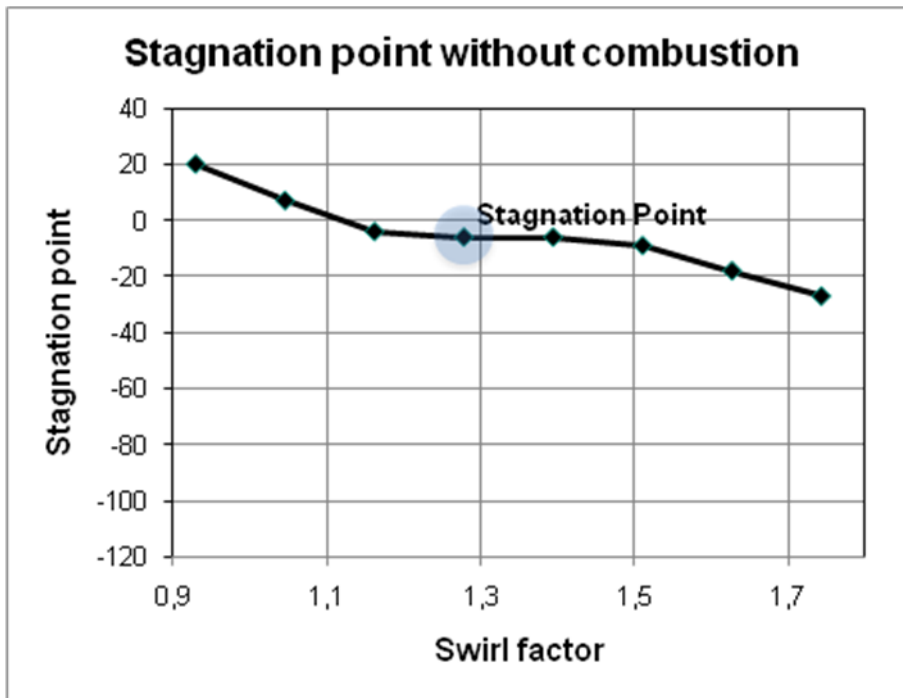


Figure 22

The vertical axis shows the axial position of the stagnation point for different swirl factors. It can be appreciated how a bigger swirl factor leads to more intense recirculation, which relocates the stagnation point upstream.

## 5.2 The reacting flow

### 5.2.1 The influence of the flame on the flow

The next step was to implement combustion in the previously mentioned model. The purpose of this was to learn more about the influence of the flame on the flow.

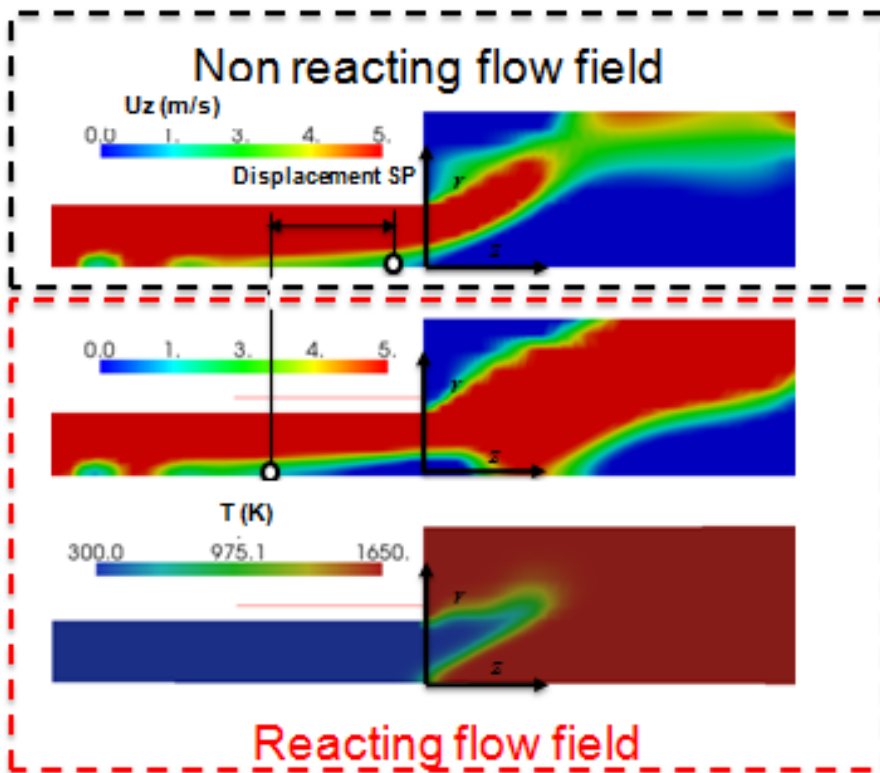


Figure 23

This is a comparison of the axial velocity fields for the cold and the reacting flow, as well as the temperature distribution in the case of combustion, which provides us with a hint as for the position and shape of the flame. The velocity scale has been adapted for better visualization of the recirculation zones. The presence of combustion relocates the stagnation point upstream for a constant swirl factor.

For better understanding, a plot of the axial velocity along the axis is shown in Figure 24:

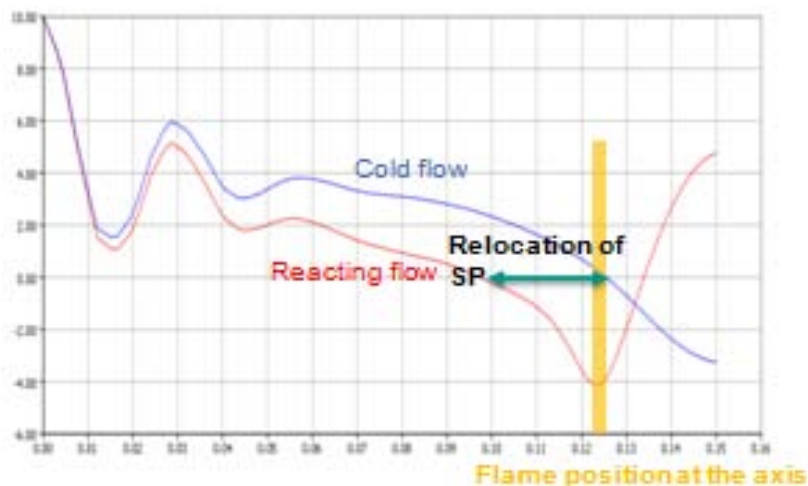


Figure 24

As can be seen, the flame not only has an influence on the flow downstream, where it accelerates the latter, but also upstream, by decelerating it.

This simulation was carried out for different swirl factors, which results were plotted together with those of the non reacting flow field, to analyse them.

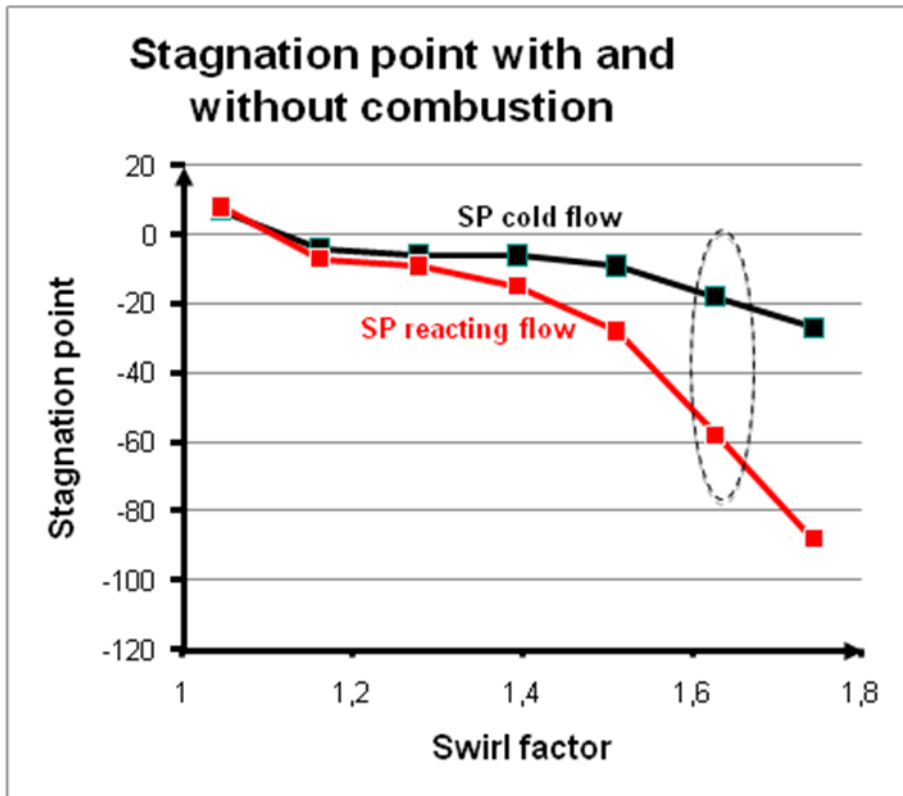


Figure 25

The dotted line surrounds the previously presented simulation. It can be seen that for swirl factors of 1,4 and above, the shift in the stagnation point is quite important.

### 5.2.2 The influence of the flow on the flame

So far the influence of the flame on the flow has been exposed. However, it must not be forgotten that there is an influence of the flow on the flame as well. In Figure 25, which is basically the previously shown diagram expanded for a broader range of swirl factors, the influence of the swirl flow, an intrinsic characteristic of the flow, is shown on the position of the stagnation point and the flame.

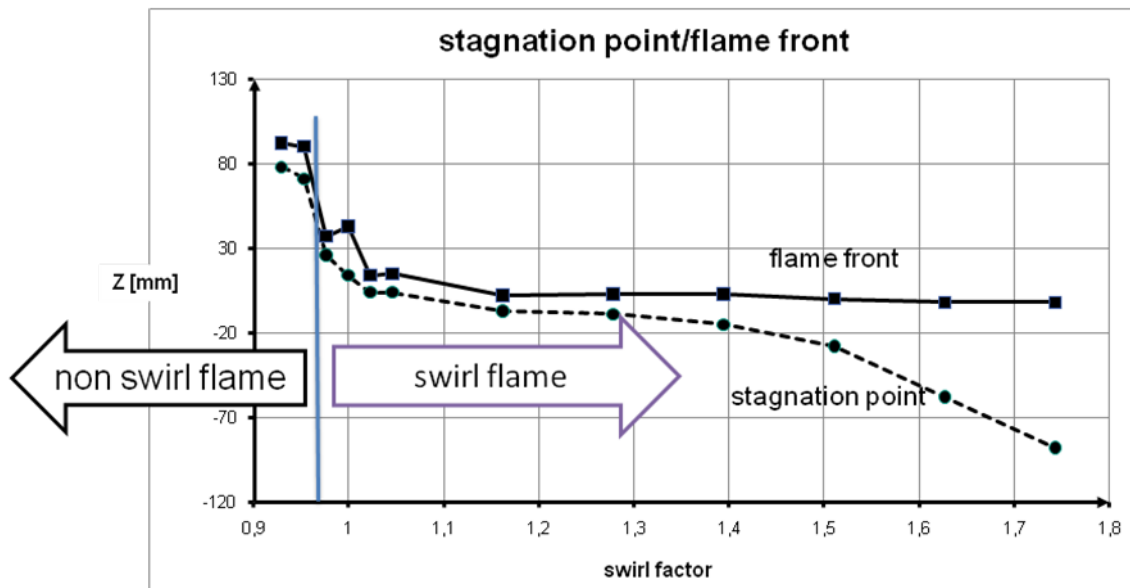


Figure 25

The influence of the swirl number on the flame goes beyond the relocation of the the flame front along the axis, since it can determine the type of flame we are talking about. For low enough swirl numbers, the flame completely changes: it stops being a swirl stabilized film to become a back step flame. This is better appreciated by zooming into the left side of the chart.

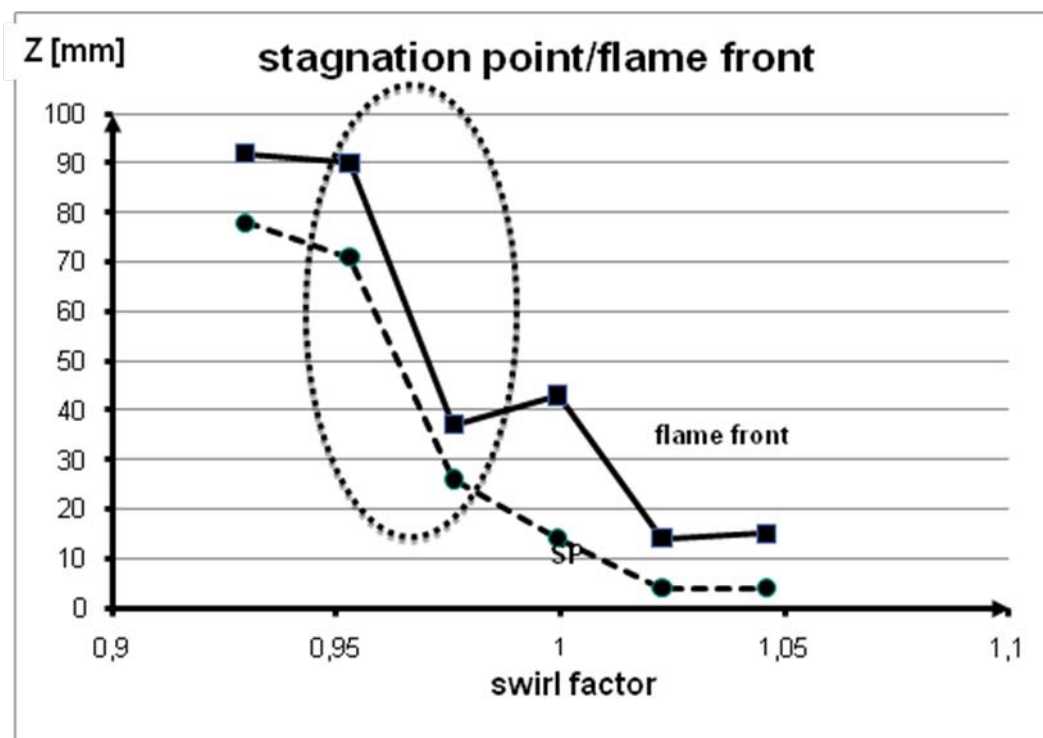


Figure 26

The transition zone is quite sudden and takes place in our simulation for swirl factor values of roundabout 0.95.

These are the axial velocity and temperature fields of both sides of the transition zone:

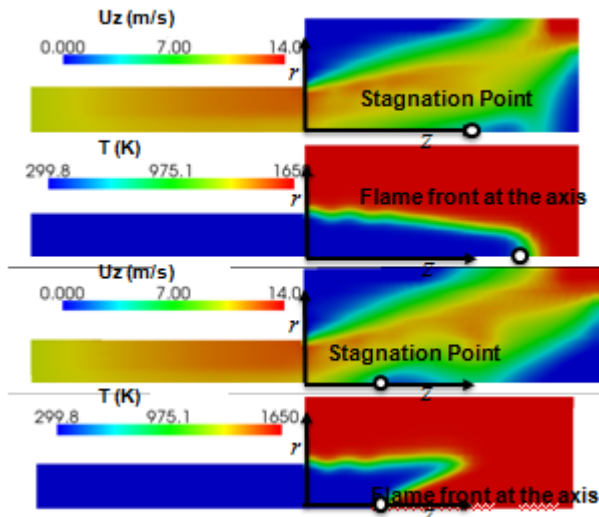


Figure 27

The upper flame is a “back step flame”, which means it is stabilized exclusively by the recirculation zone at the corner. The flame below is a “swirl stabilized flame”, in which the recirculation zone at the axis also contribute to the flame stabilization. It can be seen that besides the differences in the position of the flame, there are clear differences in the shape of the flame itself.

The flow has indeed a great influence on the flame, which we will eliminate through the fixed flame concept.

### 5.3 The fixed flame

#### 5.3.1 Checking the fixed flame concept

To be able to study the isolated influence of the flame on the flow we created a “fixed flame”. This flame is created using the “progress variable” principle, together with the corresponding initialization of the temperature. This was taken care of in a way there would be no discontinuities, all transitions take place in a gradual way.

Discontinuities were to be avoided since they reduced the stability of the simulation.

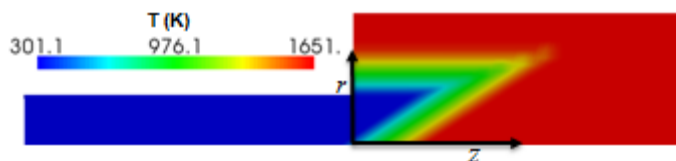


Figure 28

To be able to use this model, it was checked that the flow field in the case of the fixed flame was very similar to the one that goes along with the free flame. After a couple changes in the geometry of the fixed flame, this was achieved as can be seen in Figure 28.

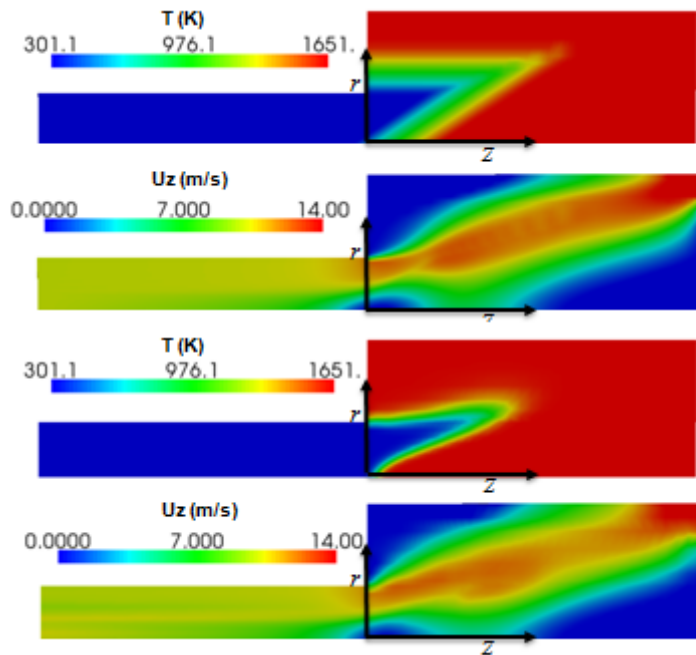


Figure 29

The velocity field in both cases is almost identical in spite of the differences in the geometry of the flame.

### 5.3.2 Modification of parameters in the fixed flame to study their influence on the flow field.

The final step was the study of the isolated influence of modifications on the flame, one at a time. We tweaked the flame front thickness and the angle between the flame front and the axis.

#### **Influence of the thickness of the flame front.**

This study was chosen because flames in which the burning velocity is greater tend to be thinner.

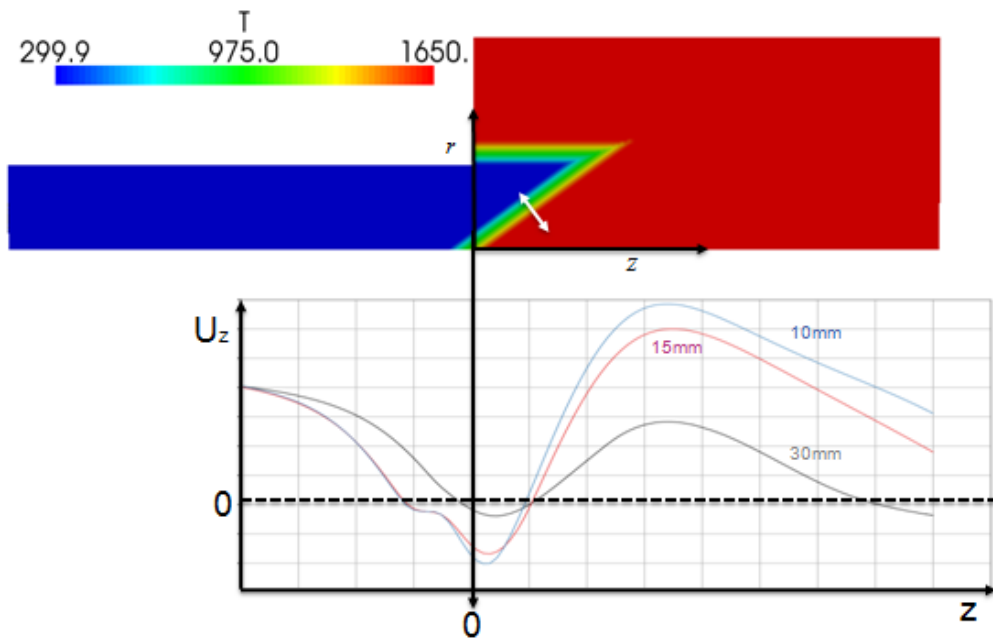


Figure 30

It can be appreciated how thinner flames cause more important decelerations (upstream from the flame) and accelerations (downstream from the flame).

**Influence of the angle between the flame front and the axis.**

This study was chosen after having observed in the simulation s than above a certain swirl factor, the flame stabilizes between the premixing zone and the combustion chamber. What changes in the flame from then on is the angle between the flame front and the axis, which grows along with the swirl factor.

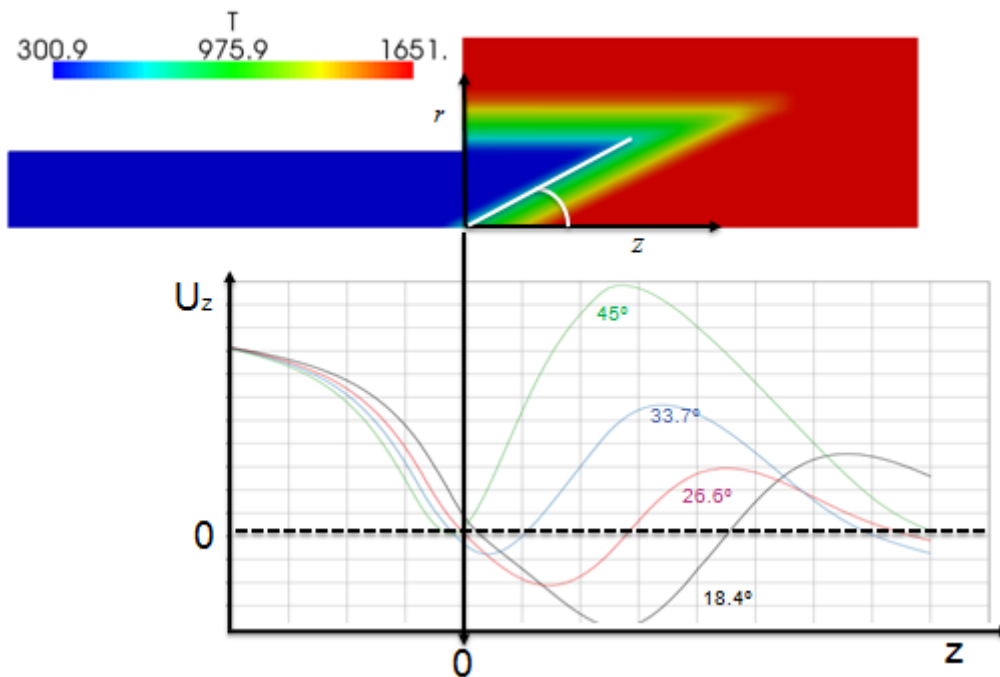


Figure 31

The bigger the angle of the flame front with the axis, the more upstream the stagnation point is relocated. The lower this angle, the stronger the recirculation is (greater negative axial velocities, for a wider range of axial positions)

## 6 Outlook

The next steps to be taken to continue with the work are the following:

- Study of the influence of the turbulence and combustion models, as well as changing the tweaking of parameters.
- Building a 3D non stationary simulation, closer to reality and therefore more accurate.

## 7 Appendix- OpenFOAM

### 7.1 The Concept of CFD in Open Foam

OpenFOAM is a C++ library, used to create the following executables (known as applications)

- *Solvers*, designed to solve a specific problem
- *Utilities*, which purpose is data manipulation

Probably the most power feature of this CFD tool is that it new solvers and utilities can be created by its users, provided they have some knowledge on the underlying method, physics, and programming.

The overall structure of OpenFOAM is as follows:

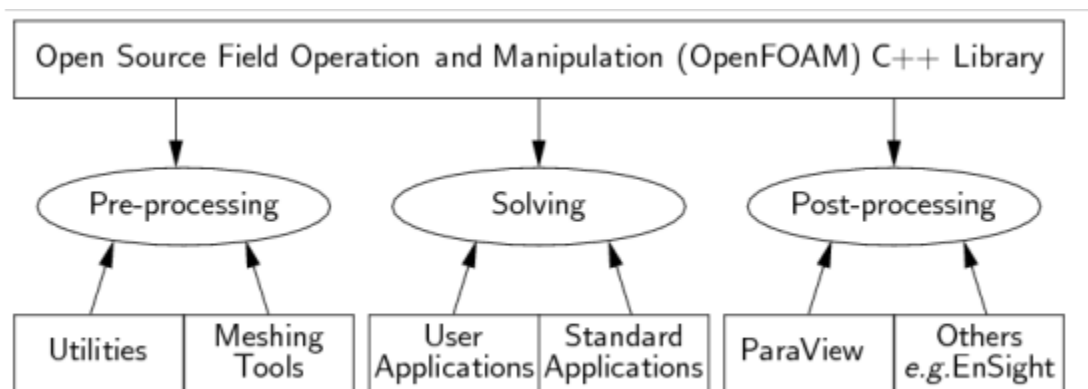


Figure 31

Pre-processing is everything that is needed to get the simulation ready to be run. First of all, the case geometry along with a mesh is needed. There are two options, both of which we tried throughout our simulations: creating the geometry and meshing inside OpenFOAM with the *blockMeshDict* file, or to import them from special meshing programs (such as *ANSYS ICEM*, which is the one we used).

The first option is quite handy for simple geometries and meshes, as was our case, otherwise it might prove a little restrictive since it is only an editable text file.

Secondly, the problem should be initialized. This means, all the boundary conditions as well as the start conditions should be set according to the user's needs.

This is all done in the first time directory.

Solving can be done in two ways: either by choosing a solver that adjusts fairly well to the user's problem (this is not too hard since there are plenty of solvers) or by modifying one of the existing solvers. Both of these procedures have been carried out.

An important aspect of OpenFOAM is that it explains itself through tutorials. There are two tutorials in the official OpenFOAM user guide which are explained thoroughly.

Besides these two, there are extremely numerous tutorials, which are missing this "detailed documented explanation", since it is considered they are "self explanatory".

Searching for the appropriate tutorial is an investment in time that pays high dividends. The user will probably find out there is a tutorial fairly similar to the problem faced, where what is needed to do is to change boundary and initial conditions here and there.

Post-processing was always done throughout this work with Paraview, open source as well. Nevertheless, OpenFOAM offers other possibilities, specially through utilities that transform the OpenFOAM data from the time directories so that they are readable by a commercial solver.

## 7.2 a rough overview on the structure of an Open Foam simulation

The file structure of OpenFOAM cases is as follows:

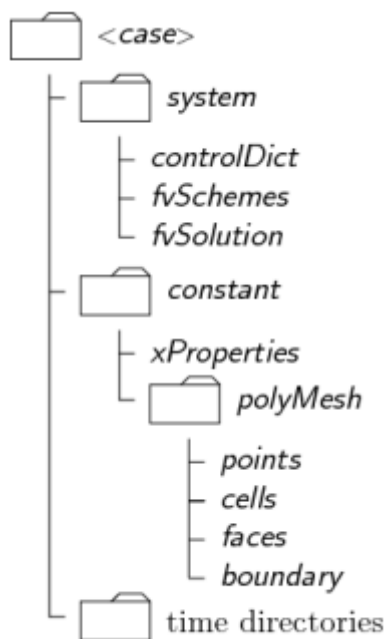


Figure 32.

- **A constant directory**  
that contains a full description of the case mesh in a subdirectory polyMesh and files specifying physical properties for the application concerned, e.g.transportProperties.
- **A system directory**  
for setting parameters associated with the solution procedure itself. It contains at least the following 3 files: controlDict where run control parameters are set including start/end time, time step and parameters for data output; fvSchemes where discretisation schemes used in the solution may be selected at run-time; and, fvSolution where the equation solvers, tolerances and other algorithm controls are set for the run.

- **The ‘time’ directories**  
containing individual files of data for particular fields. The data can be: either, initial values and boundary conditions that the user must specify to define the problem; or, results written to file by OpenFOAM. Note that the OpenFOAM fields must always be initialised, even when the solution does not strictly require it, as in steady-state problems.

### 7.3 Combustion Simulation in Open Foam- The flame in XiFoam

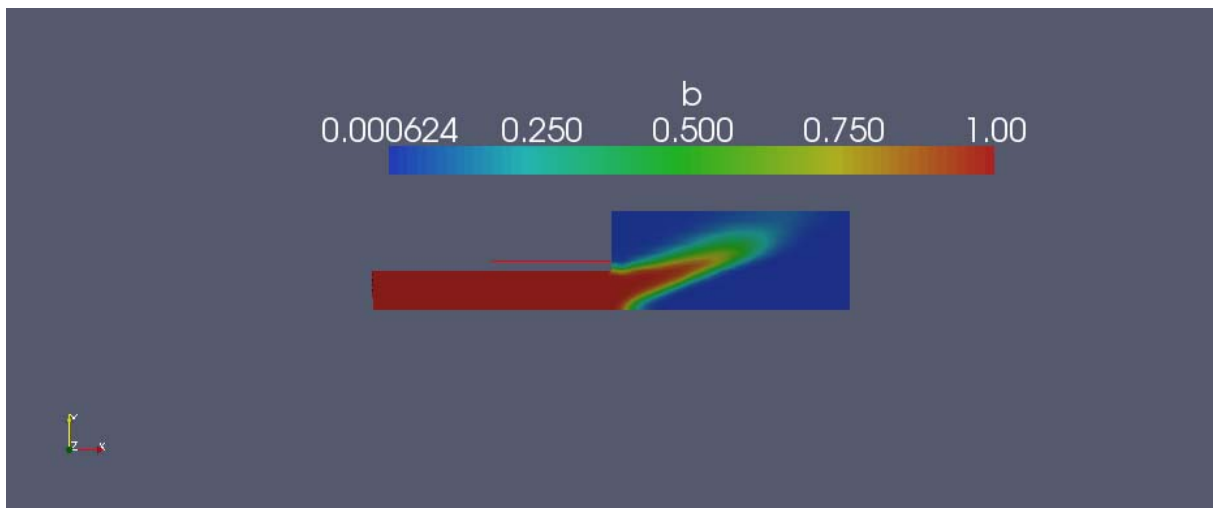


Figure 33.

In XiFoam, combustion is modelled through a “progress variable”  $b$ , which stands for the progress of the combustion.

$b=1$  means the fluid is completely unburnt,  $b=0$  means the fluid is totally burnt. Along the flame front, there is a  $b$  gradient.

These are the folders inside the *XiFoam* solver (*mixXiFoam* in this case, modified by the user)

Name	Size	File Type	Modified	Permissions	Owner
Make	4,0 KB	Folder	18-05-10 16:22	drwxr-xr-x	trejo
hEqn.H	234 B	C++ Header File	17-05-10 19:31	-rwxr-xr-x	trejo
UEqn.H	243 B	C++ Header File	17-05-10 19:31	-rwxr-xr-x	trejo
ftEqn.H	413 B	C++ Header File	17-05-10 19:31	-rwxr-xr-x	trejo
huEqn.H	523 B	C++ Header File	17-05-10 19:31	-rwxr-xr-x	trejo
readCombustionProperties.H	883 B	C++ Header File	17-05-10 19:31	-rwxr-xr-x	trejo
pEqn.H	1,3 KB	C++ Header File	17-05-10 19:31	-rwxr-xr-x	trejo
createFields.H	2,8 KB	C++ Header File	17-05-10 19:31	-rwxr-xr-x	trejo
mixXiFoam.C	4,2 KB	C++ Source File	17-05-10 19:31	-rwxr-xr-x	trejo
bEqn.H	6,6 KB	Backup File	17-05-10 20:12	-rwxr-xr-x	trejo
bEqn.H	6,8 KB	C++ Header File	18-05-10 16:21	-rwxr-xr-x	trejo
mixXiFoam.dep	38,5 KB	Plain Text Document	18-05-10 16:22	-rw-r--r--	trejo

Figure 34.

The first four contain the equations governing their respective fields

*hEqn*- enthalpy of the burnt mixture

```
fvScalarMatrix hEqn
(
    fvm::ddt(rho, h)
    + mvConvection->fvmDiv(phi, h)
    - fvm::laplacian(turbulence->alphaEff(), h)
    ==
    DpDt
);
hEqn.relax();
hEqn.solve();

thermo.correct();
}
```

Figure 35.

*huEqn*- enthalpy of the unburnt mixture

```
if (ign.ignited())
{
    solve
    (
        fvm::ddt(rho, hu)
        + mvConvection->fvmDiv(phi, hu)
        - fvm::laplacian(turbulence->alphaEff(), hu)

        // These terms cannot be used in partially-premixed combustion due to
        // the resultant inconsistency between ft and hu transport.
        // A possible solution would be to solve for ftu as well as ft.
        //- fvm::div(muEff*fvc::grad(b)/(b + 0.001), hu)
        //+ fvm::Sp(fvc::div(muEff*fvc::grad(b)/(b + 0.001)), hu)

        ==
        DpDt*rho/thermo.rhou()
    );
}
```

Figure 36.

However, it is assumed the mixture is perfectly mixed and thus it is premixed combustion

*UEqn*- velocity equation

```

fvVectorMatrix UEqn
(
    fvm::ddt(rho, U)
  + fvm::div(phi, U)
  + turbulence->divDevRhoReff(U)
  ==
    rho*g
);

UEqn.relax();

if (momentumPredictor)
{
    solve(UEqn == -fvc::grad(p));
}

```

Figure 37

*ftEqn*- fuel fraction

```

mp<fv::convectionScheme<scalar> > mvConvection
(
    fv::convectionScheme<scalar>::New
    (
        mesh,
        fields,
        phi,
        mesh.divScheme("div(phi,ft_b_h_hu)")
    )
);

if (composition.contains("ft"))
{
    volScalarField& ft = composition.Y("ft");

    solve
    (
        fvm::ddt(rho, ft)
      + mvConvection->fvmDiv(phi, ft)
      - fvm::laplacian(turbulence->alphaEff(), ft)
    );
}

```

Figure 38.

The *readCombustionProperties* folder reads, as its name says, some combustion properties, which have to be given as input by the user to initialize the calculations, otherwise it takes default values from its corresponding tutorial. These properties change in time.

```

Info<< "Reading combustion properties\n" << endl;

IOdictionary combustionProperties
(
    IObject
    (
        "combustionProperties",
        runTime.constant(),
        mesh,
        IOobject::MUST_READ,
        IOobject::NO_WRITE
    )
);

word SuModel
(
    combustionProperties.lookup("SuModel")
);

dimensionedScalar sigmaExt
(
    combustionProperties.lookup("sigmaExt")
);

word XiModel
(
    combustionProperties.lookup("XiModel")
);

dimensionedScalar XiCoef
(
    combustionProperties.lookup("XiCoef")
);

dimensionedScalar XiShapeCoef
(
    combustionProperties.lookup("XiShapeCoef")
);

dimensionedScalar uPrimeCoef
(
    combustionProperties.lookup("uPrimeCoef")
);

ignition ign(combustionProperties, runTime, mesh);

```

Figure 39.

Out of these values, there are to be pointed out  $Su$ , the laminar flame speed,  $Xi$ , the flame wrinkling, and *ignition*, which can be turned off (to compare with a cold-flow field, for instance).

The *pEqn* folder is similar to the ones seen above.

Concerning the flame, “most of the action” takes place in the *bEqn* folder.

All the coefficients in the *readCombustionProperties* folder are calculated in this one. The *b* equation itself is as follows:

```

// Create b equation
// ~~~~~
fvScalarMatrix bEqn
(
    fvm::ddt(rho, b)
  + mvConvection->fvmDiv(phi, b)
  + fvm::div(phiSt, b, "div(phiSt,b)")
  - fvm::Sp(fvc::div(phiSt), b)
  - fvm::laplacian(turbulence->alphaEff(), b)
);

```

Figure 40

The temperature is calculated in a rather simplistic way, with a folder outside the solver (inside the *system* folder) called *setFieldsDict*

```

defaultFieldValues
(
    volScalarFieldValue b 1
    volScalarFieldValue T 293
);

regions
(
    boxToCell
    {
        box (-1 -1 -1) (1 0 1);
        fieldValues
        (
            volScalarFieldValue b 0
            volScalarFieldValue T 1650
        );
    }
);

```

Figure 41.

What it does is set the temperature  $T$  to a certain value wherever  $b$  equals 0. This may not be the most realistic way to calculate temperature, but it is very lean in resources, and since the focus of this study is not to concentrate on chemical reactions and temperature but on the flow field, it was thought it suited its needs.

The first part of the loop is calculating all the above mentioned values. These serve as input for the *XiFoam.C* folder, the solver itself.

```

// --- Pressure-velocity PIMPLE corrector loop
for (int oCorr=0; oCorr<nOuterCorr; oCorr++)
{
    #include "rhoEqn.H"
    #include "UEqn.H"

    #include "ftEqn.H"
    #include "bEqn.H"
    #include "huEqn.H"
    #include "hEqn.H"

    if (!ign.ignited())
    {
        hu == h;
    }

    // --- PISO loop
    for (int corr=1; corr<=nCorr; corr++)
    {
        #include "pEqn.H"
    }

    turbulence->correct();
}

rho = thermo.rho();

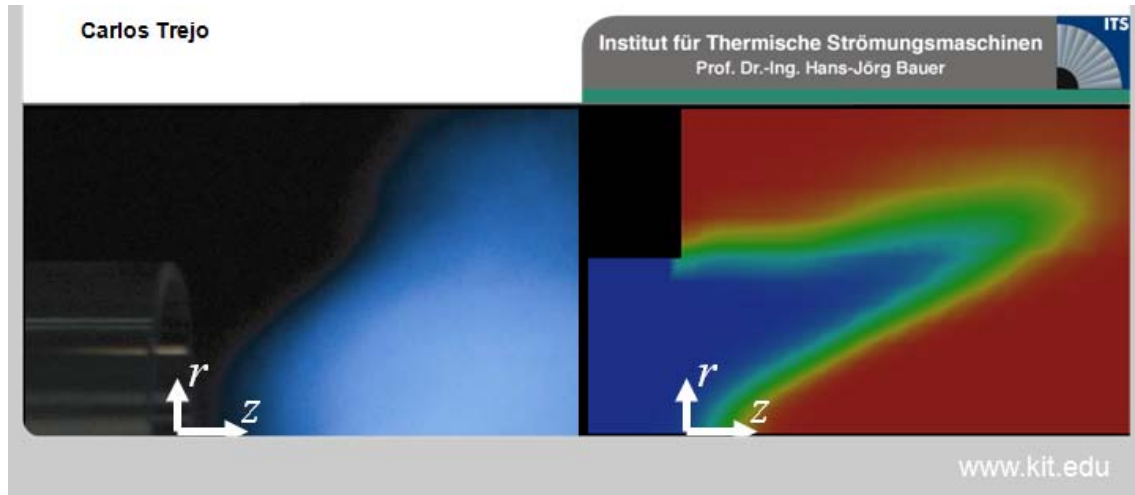
runTime.write();

```

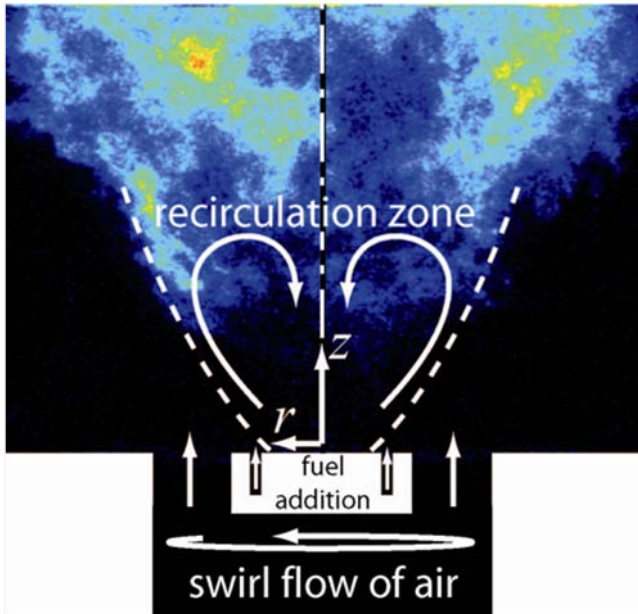
Figure 42.

The density  $\rho$  is read from a table which takes into account the temperature, and is used to recalculate the other variables, which will serve as input in the next time step.

# Simulación de la Influencia Aerodinámica de Combustión en Flujos Rotacionales.



# 1 La influencia aerodinámica de la combustión. Qué se quiso aprender acerca de ella y por qué.



Llama no premezclada con flujo rotacional, estabilizada con un cuerpo central [Keck and Aigner 2001]

Figura 1

La rotación con la cual entra el flujo a la entrada de esta llama origina las zonas de recirculación que pueden verse en la Figura , donde se puede observar, que la posición de la llama y la zona de recirculación están estrechamente liadas.

Para implementar mejoras a esta llama, es necesario entender la interacción entre el flujo y la llama. Esta interacción está ilustrada en la Figura

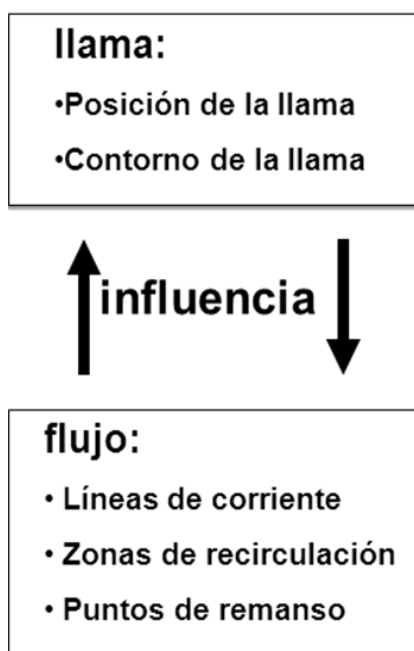


Figura 2

No sólo la llama tiene una influencia sobre el flujo, modificando líneas de corriente, zonas de recirculación, y puntos de remanso. También existe un efecto de realimentación del flujo sobre la llama. Aquí está la complejidad del problema.

La llama anteriormente presentada es una llama no premezclada, muy parecida a aquellas que pueden ser observadas en turbinas de gas.

Para reducir emisiones, en el futuro las llamas deberían ser premezcladas. En las llamas premezcladas, hay una zona de mezcla en la cual el combustible se mezcla con el oxidante, antes de quemar.

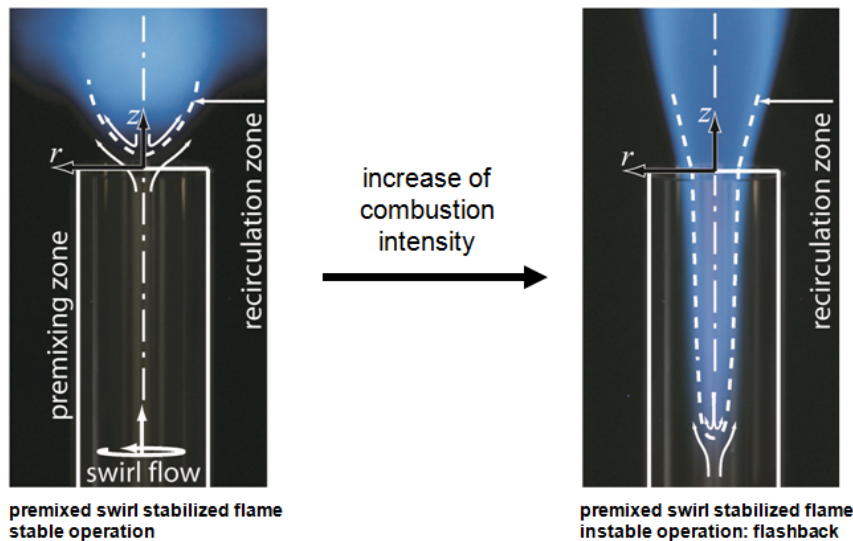


Figura 3

Como se puede apreciar en la Figura , un aumento en la intensidad de la combustión puede llevar a la llama, estabilizada en un momento tras la zona de premezcla, a reubicarse dentro de esta zona, cambiando completamente de estructura. Este fenómeno es conocido como Flashback, y en la práctica, puede ocasionar la destrucción del sistema de combustión. Flashback ha sido lo que nos ha motivado a aprender más sobre la interacción entre la llama y el flujo.

## 2 Estrategia para aprender: un modelo de simulación numérica

Este proyecto cumple la función de reforzar y comprobar ciertas teorías extraídas de un experimento llevado a cabo en el “Institut für thermische Strömungsmaschinen” del “Karlsruhe Institut of Technology”, por el Ing. Georg Blessinger.

El objetivo era de obtener predicciones correctas cualitativamente de la interacción entre el flujo y la llama para diferentes situaciones. Como se verá más tarde, se estuvo caminando sobre terreno desconocido, con lo cual un mecanismo de aprendizaje fue “ensayo y error”. Esto requiere simular una gran cantidad de veces, lo cual sólo es posible si éstas tienen duraciones relativamente cortas. No era necesaria una herramienta especialmente precisa, sino una más bien rápida.

Es por eso que se escogió un modelo en dos dimensiones, RANS (Reynolds Averaged Navier Stokes) y un mallado relativamente grueso.

## Procedimiento:

1. Modelización del flujo sin combustión
2. Modelización del flujo con combustión, con una llama libre
3. Modelización del flujo con combustión, con una llama fija (sin influencia del flujo sobre la llama)

flujo

flujo ↔ llama

flujo ← llama

El primer paso fue la modelización del flujo sin combustión. A continuación, este modelo fue extendido, y en él se introdujo combustión. El problema de este experimento, es que era imposible aislar la influencia de la llama sobre el flujo, ya que el flujo no sólo era modificado por la llama, sino que también tenía una influencia de tipo realimentación sobre la misma. Se decidió romper este bucle de realimentación. Esto fue posible modificando el código del “solver”, de manera que la llama permaneciera fija en el espacio. Tras ser inicializada de acuerdo con nuestras necesidades, esta llama permanecía intacta a lo largo de la simulación, lo que elimina la influencia del flujo en la llama.

## 2.1 Caracterización del flujo

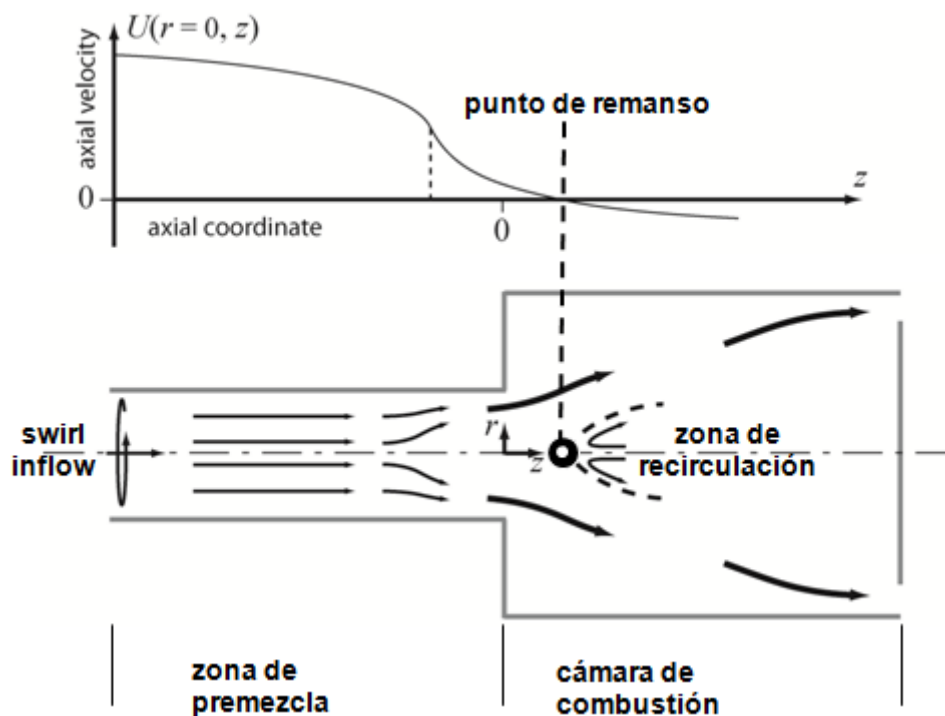


Figura 4

La geometría del problema, bastante simple, consiste de dos cilindros: la zona de premezcla, y la cámara de combustión. El flujo, que entra con una cierta rotación la zona de premezcla, sufre una expansión radial al llegar a la cámara de combustión, creando una zona de recirculación en torno al eje.

En la distribución de velocidades axiales a lo largo del eje, se puede distinguir el punto de remanso, punto para el cual la velocidad axial es nula. Este punto marca el comienzo de la zona de recirculación, y será el parámetro que emplearemos para caracterizar el flujo.

## 2.2 Caracterización de las llamas

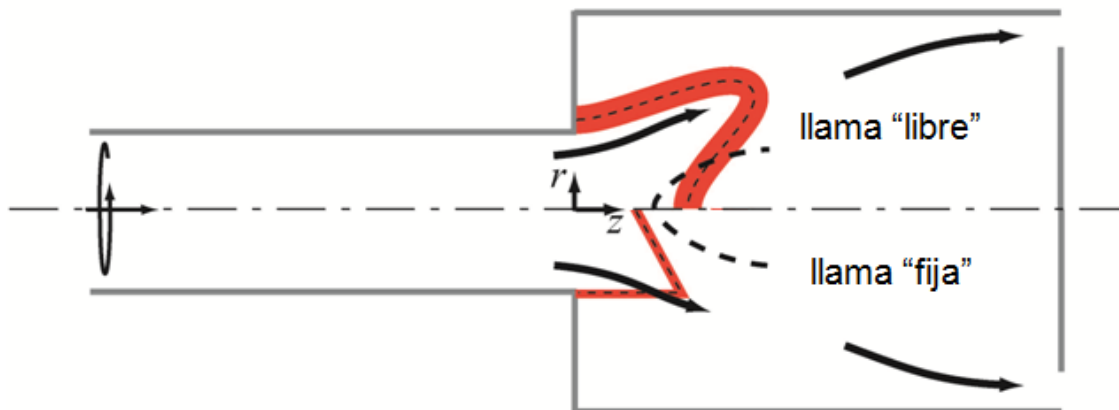


Figura 5

Como fue mencionado anteriormente en este estudio se ha trabajado con dos tipos de llamas: la llama natural, que se adapta al flujo, y la llama fija, sobre la cual ejercemos un control absoluto. En esta llama podemos cambiar ciertos parámetros para estudiar su influencia, como la posición axial, el espesor del frente de llama, y el ángulo que forma éste con el eje.

## 3 Configuración del experimento numérico

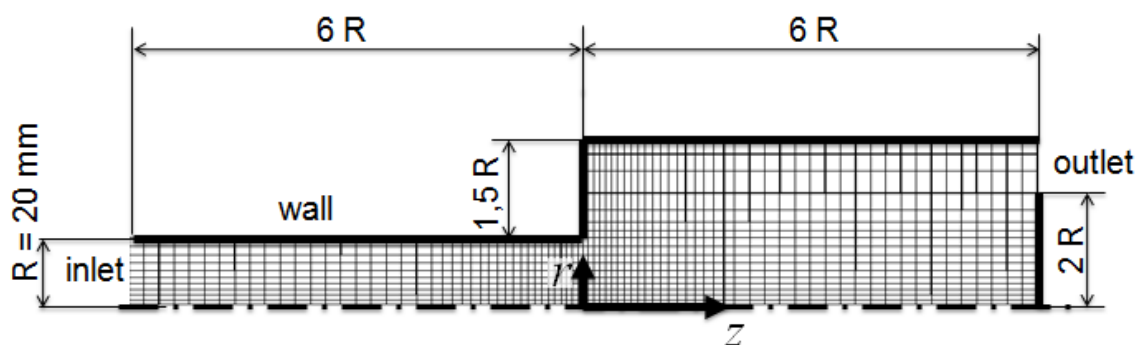


Figura 6

Se escogió hacer una simplificación axisimétrica en 2D de la geometría, y he aquí el mallado. Ciertas zonas, véase el eje o el codo, requerían una mayor precisión de mallado. En estos puntos, el mallado fue refinado consecuentemente. Para mayor estabilidad de la simulación, se escogió una pared a la salida, como es costumbre en este tipo de simulaciones, ya que el flujo inverso que puede ocurrir en estos puntos contribuye negativamente a la estabilidad del problema.

El código CFD (computational fluid dynamics) escogido fue OpenFOAM, un programa en código abierto que como tal, permite modificaciones en el código, lo cual era de crucial

importancia. El “solver” ha sido XiFoam a lo largo del estudio, un solver compresible que contempla combustión con ayuda de una “variable de progreso”.

El modelo turbulento escogido fue RAS (Reynolds Averaged Stress), que resuelve las ecuaciones para el flujo medio y hace la estadística de las fluctuaciones. El modelo de combustión empleado fue “Weller Flame Surface Density model”, que tiene en cuenta la mayor superficie de una llama “instantánea” debida al “wrinkling” de la llama o arrugamiento.

Las condiciones de contorno fueron escogidas de la siguiente manera (he aquí las más relevantes):

	Inlet	Walls	Outlet
Velocity	Rankine vortex	Slip	zeroGradient
Pressure	zeroGradient	zeroGradient	102000 Pa
Temperature	300K	zeroGradient	zeroGradient

La velocidad a la entrada consta de dos componentes: componente axial y componente radial, que tiene la forma a lo largo del radio de un vórtice de Rankine.

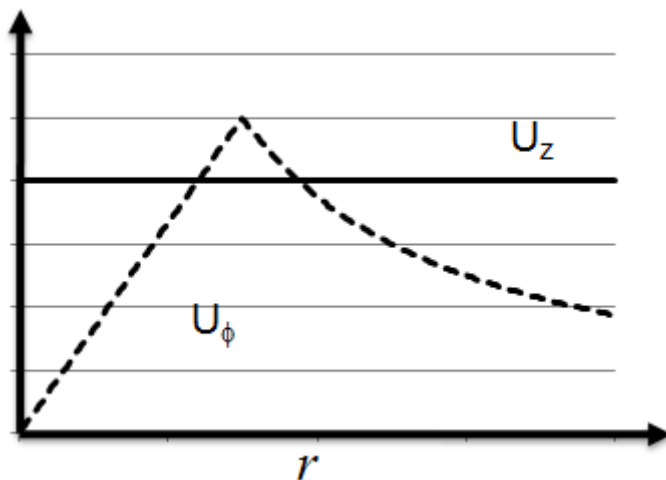


Figura 7

La temperatura fue fijada a la entrada, la presión a la salida.

## 4 Influencia aerodinámica observada

### 4.1 Modelización del flujo sin combustión

El primer paso fue la modelización del flujo sin combustión. En la Figura se puede ver la velocidad axial. La escala ha sido escogido con el objeto de poder apreciar las zonas de recirculación: azul significa velocidades axiales de 0m/s o negativas.

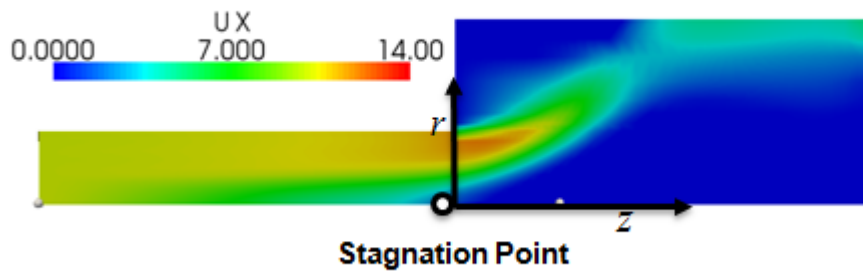


Figura 8

Existen dos zonas de recirculación, una en la esquina, y otra en el eje, que es la que nos interesa. El punto de remanso (Stagnation Point) precede esta zona de recirculación. El “swirl factor” es un parámetro bastante frecuente en este tipo de experimentos para cuantificar la cantidad de rotación lleva el flujo. Se define como el ratio entre la el flujo de cantidad de movimiento rotacional, y el flujo de cantidad de movimiento axial

$$S = \frac{\dot{D}}{I}$$

Este experimento ha sido llevado a cabo para diferentes “swirl factors”, cuyos resultados caracterizados por el punto de remanso se pueden ver en la siguiente gráfica:

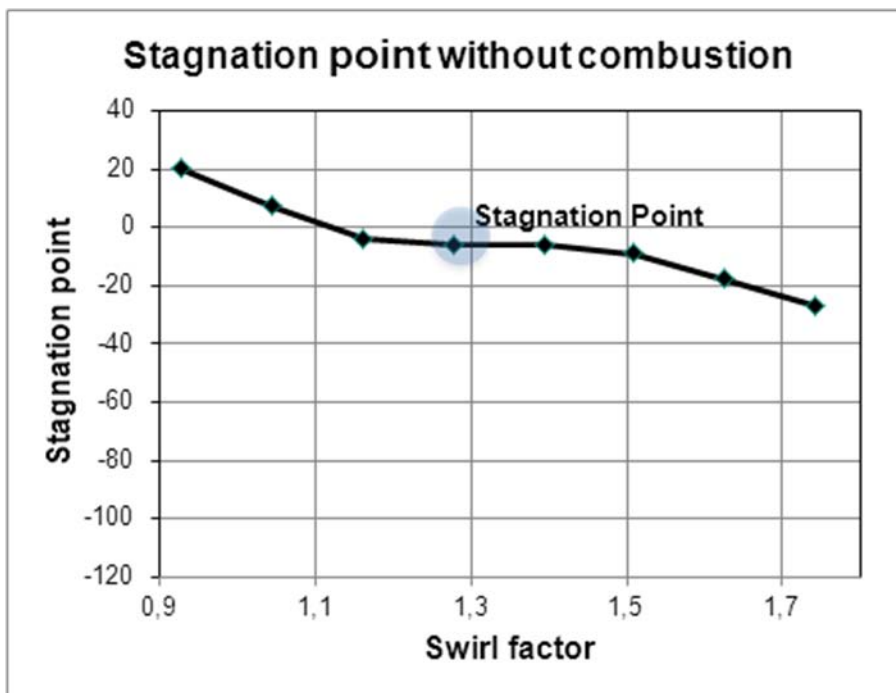


Figura 9

El eje vertical indica la coordenada axial del punto de remanso. Se puede apreciar como una mayor rotación “swirl” del flujo causa una recirculación más intensa, lo cual recoloca el punto de remanso aguas arriba.

## 4.2 Implementación de la combustión

### 4.2.1 El efecto de la llama sobre el flujo

El siguiente paso fue implementar la combustión en el modelo. Con ello, teníamos como objetivo estudiar la influencia de la llama sobre el flujo.

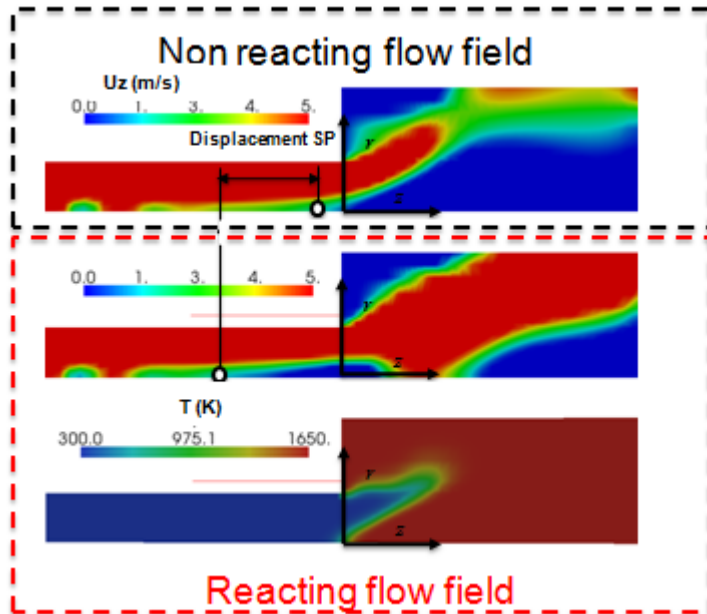


Figura 10

En la Figura se pueden ver las distribuciones de velocidad axial para el sin y con combustión, así como el campo de temperaturas del caso con combustión, que nos da una idea de la posición y forma de la llama. La escala para las velocidades está adaptada para una mejor visualización de las zonas de recirculación. Se puede apreciar que la presencia de la combustión sitúa el punto de remanso aguas arriba, para un mismo “swirl number”. Para una mejor ilustración de esto, se ha incluido la velocidad axial a lo largo del eje:

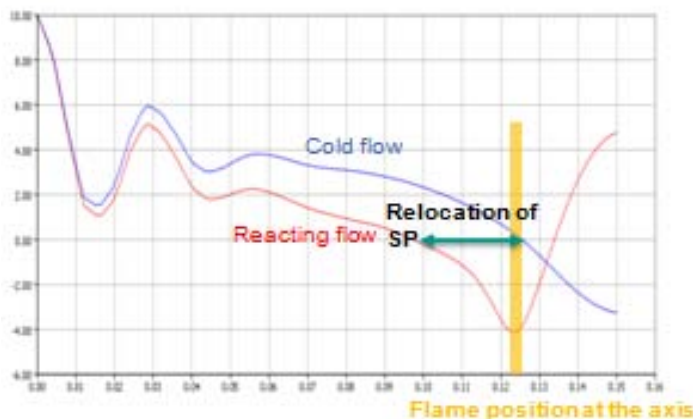


Figura 11

La llama no sólo tiene una influencia aguas abajo, acelerando el flujo, también aguas arriba, frenándolo.

Esta simulación se llevó a cabo para diversos “swirl factors”:

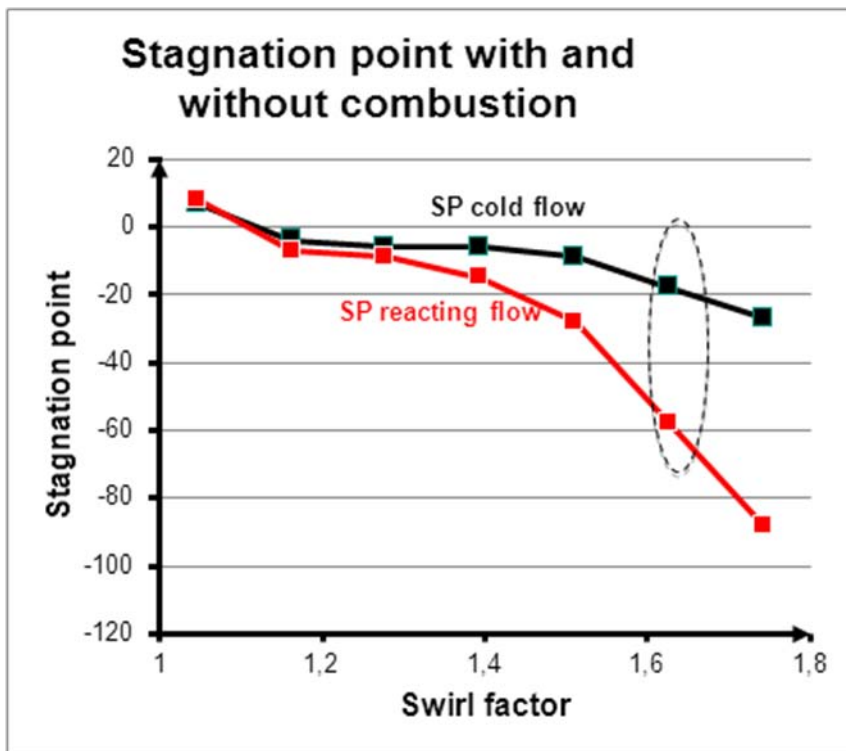


Figura 12

La línea punteada indica la simulación anteriormente presentada. Se puede apreciar que para swirl factors de más de 1,4 la el punto de remanso sufre una importante relocalización.

#### 4.2.2 Efecto realimentación del flujo sobre la llama

En la figura se puede apreciar la influencia del swirl flow, característica intrínseca del flujo, sobre la posición axial del punto de remanso y de la llama

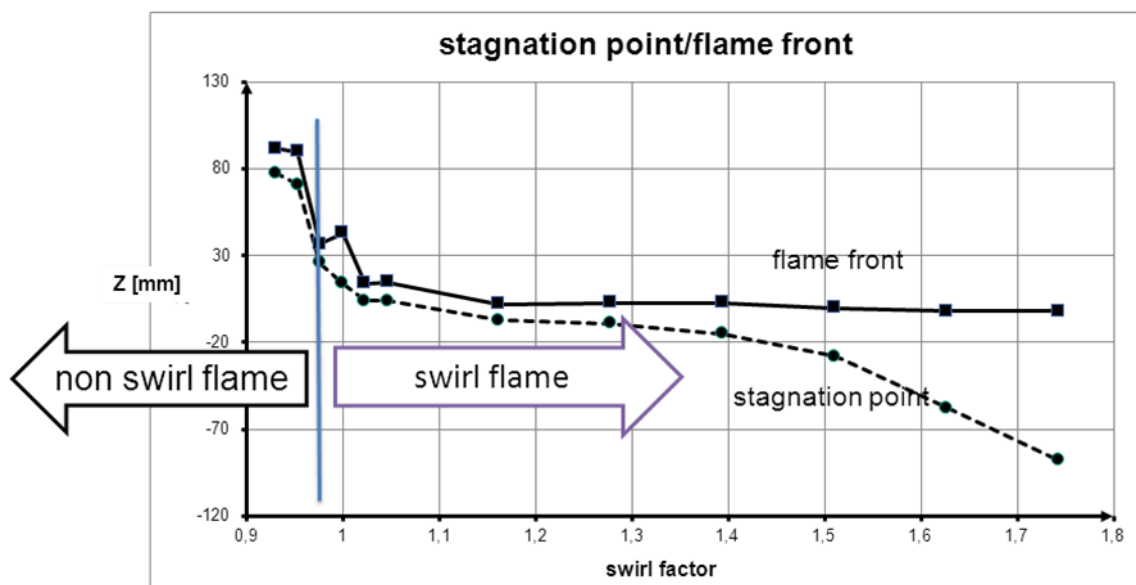


Figura 13

Hay también una influencia sobre la posición de la misma, no sólo esto sino que para swirl factors suficientemente bajos la llama cambia de tipo por completo y deja de ser una "swirl

stabilized flame”. Esto se aprecia mejor haciendo un zoom a la izquierda del diagrama, a la zona de transición entre las dos llamas.

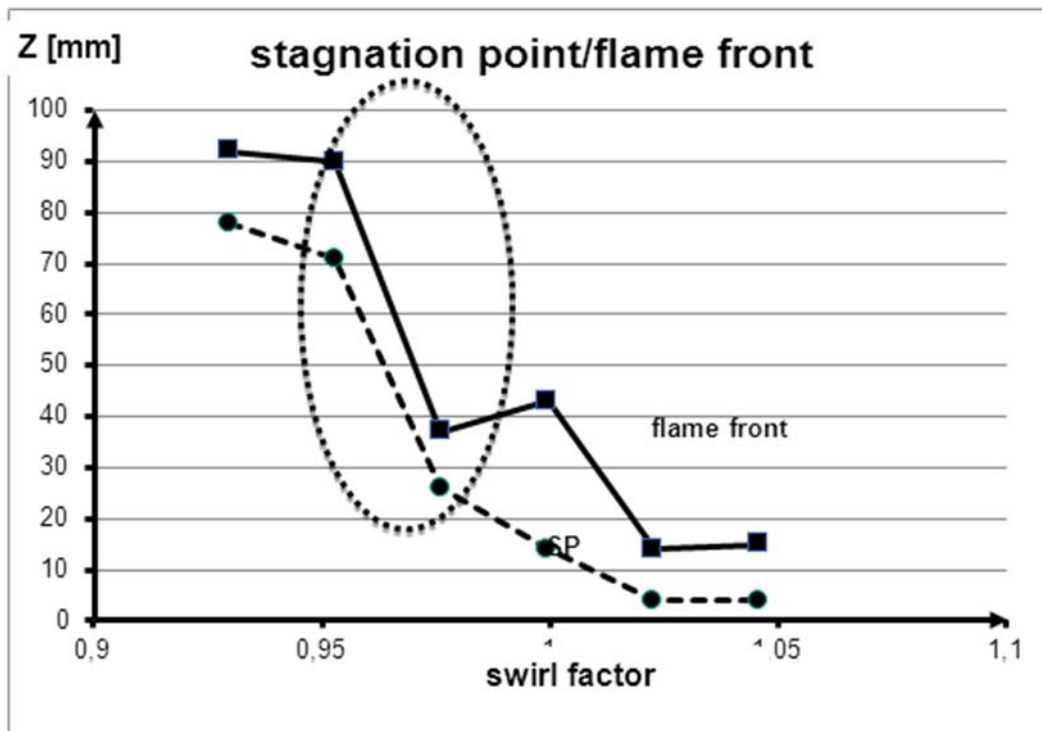


Figura 14

La zona de transición es brusca y tiene lugar en el caso de nuestro experimento para valores de swirl factor de en torno a 0.95.

A continuación se muestran los campos de velocidades axiales y de temperaturas a ambos lados de la transición

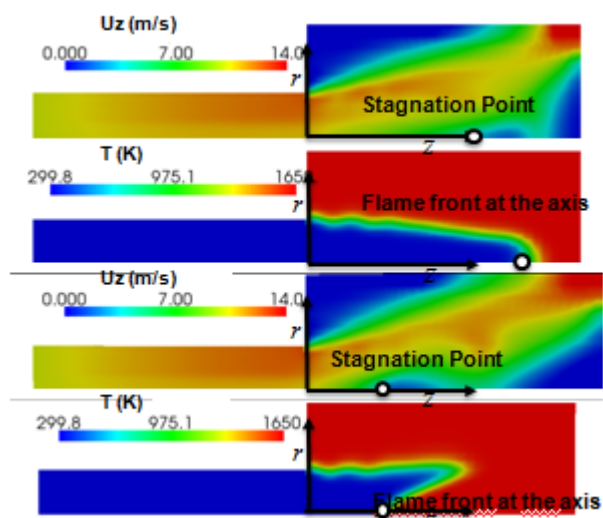


Figura 15

La llama de arriba es de tipo “back step flame”, no estabilizada por la recirculación del eje sino por aquella de la esquina. En la de abajo, una “swirl stabilized flame”, la zona de recirculación del eje también contribuye a estabilizar la llama. Se puede ver que a parte de la diferente posición de la llama, también hay una diferencia en la constitución de la misma, su

forma es muy distinta. Esto nos muestra, que el flujo tiene efectivamente una gran influencia en la llama, influencia que vamos a eliminar a través del concepto “llama fija”

### 4.3 La llama fija

#### 4.3.1 Validación del concepto de llama fija

Para poder estudiar la influencia aislada de la llama sobre el flujo hemos creado una “llama fija”. Esta llama está creada utilizando el principio de la “variable de progreso” junto con una inicialización de la temperatura, ambas de forma que no haya discontinuidades, las cuales restan estabilidad al problema.

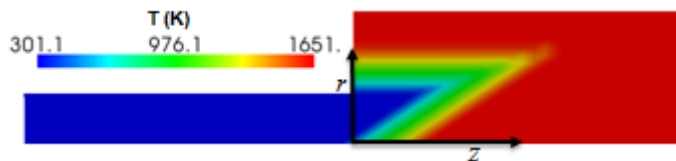


Figura 16

Para poder utilizar este modelo, se verificó que el flujo asociado a una llama fija era muy similar al de una llama libre. Tras un par de cambios en la geometría de la llama fija, esto fue logrado, como se puede ver en la figura

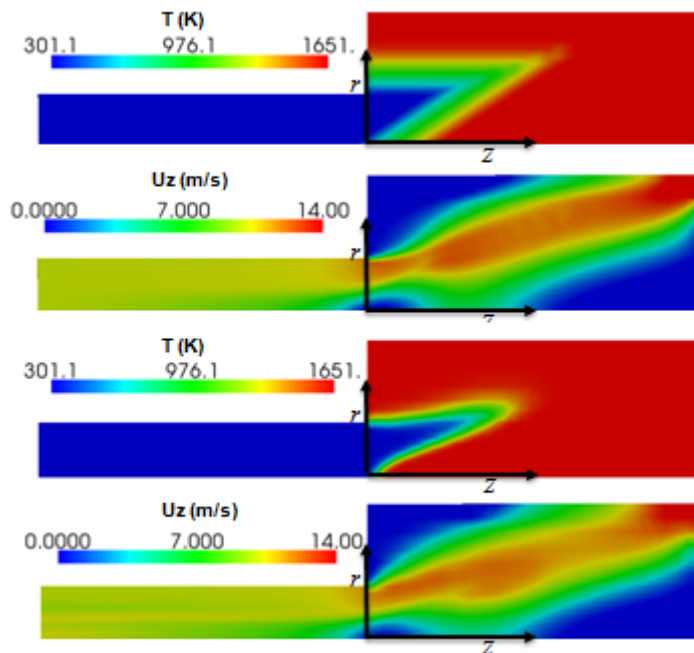


Figura 17

El campo de velocidades en ambos casos es casi idéntico, a pesar de la diferencias en la geometría de la llama.

### 4.3.2 Modificación de parámetros de la llama fija para el estudio de su influencia sobre el flujo

El paso final fue el estudio de la influencia aislada de modificaciones a la llama, una por una. Se hicieron modificaciones en el espesor de la llama, así como en el ángulo que ésta forma con el eje.

#### 4.3.2.1 Influencia del espesor del frente de llama.

Este estudio se escogió pues llamas en las cuales la velocidad de combustión es mayor tienden a ser más finas.

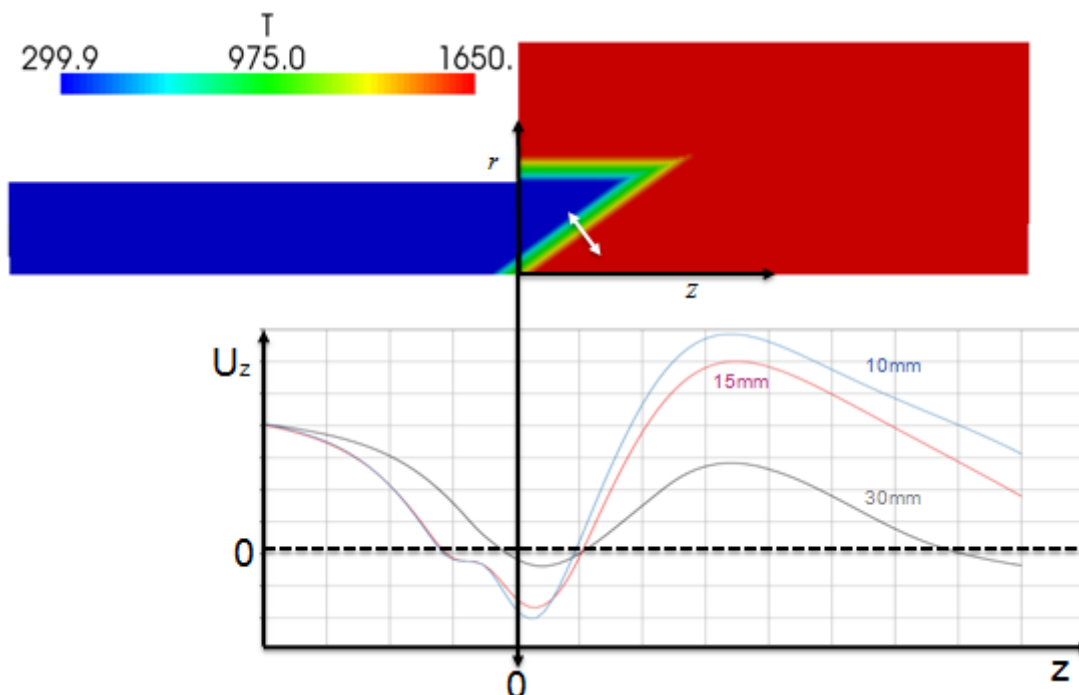


Figura 18

Se puede apreciar como llamas más finas son causantes de deceleraciones (aguas arriba de la llama) y aceleraciones (aguas debajo de la llama) más importantes.

#### 4.3.2.2 Influencia del ángulo del frente de llama con el eje

Este estudio se escogió pues se constató a través de las simulaciones que a partir de un cierto swirl factor, la llama se estabiliza entre la zona de premezcla y la cámara de combustión. Lo que cambia de la llama es el ángulo de ésta, que crece junto con el swirl factor.

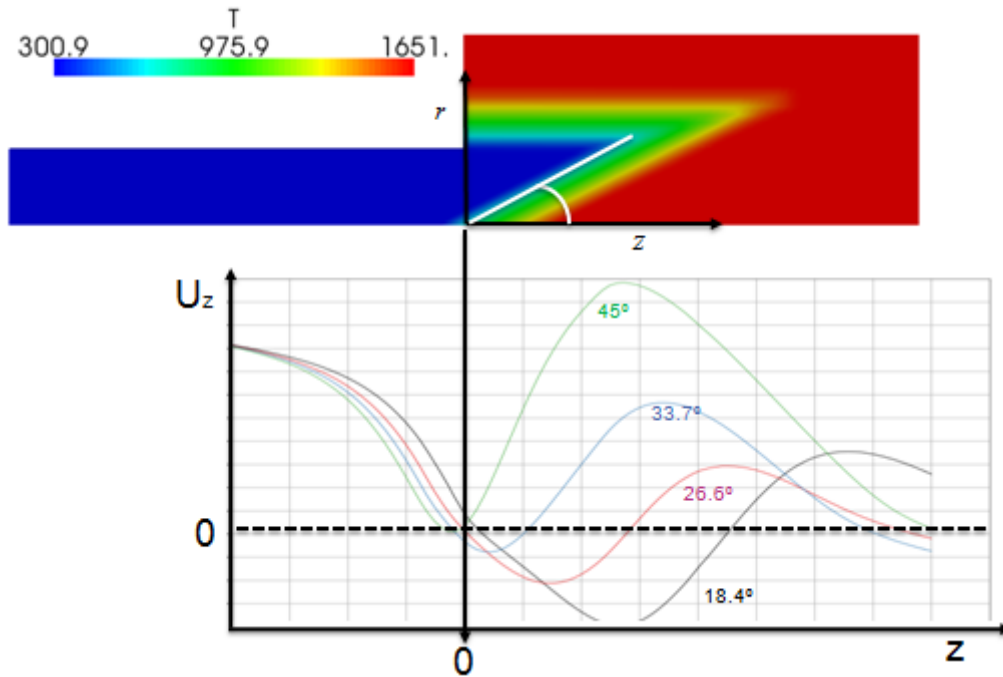


Figura 19

A mayor ángulo de la llama con el eje, más aguas arriba se sitúa la zona de recirculación, a menor ángulo, mayor es la recirculación.

#### 4.4 Continuación de este trabajo

Los siguientes pasos a tomar para continuar el estudio serían:

- Estudio de la influencia del modelo de turbulencia y de combustión, así como de sus respectivos parámetros
- Concepción de una simulación 3D con un modelo no estacionario